Molecular modelling of wetting behaviour

Martin Horsch,[1, 4] Stefan Becker,[1] Juan Castillo,[1] Felix Diewald,[2] Michaela Heier,[1] Maximilian Kohns,[1] Simon Stephan,[1] Ralf Müller,[2] Herbert Urbassek,[3] and Hans Hasse[1]

[1]Engineering Thermodynamics, [2]Applied Mechanics, [3]Computational Materials Science, University of Kaiserslautern, Germany,
[4]Chemical Engineering, IIT Kanpur, India

Computational
Molecular Engineering

Chemical Engineering Seminar
IIT Bombay, January 25, 2017

Molecular modelling of wetting behaviour and self assembly …

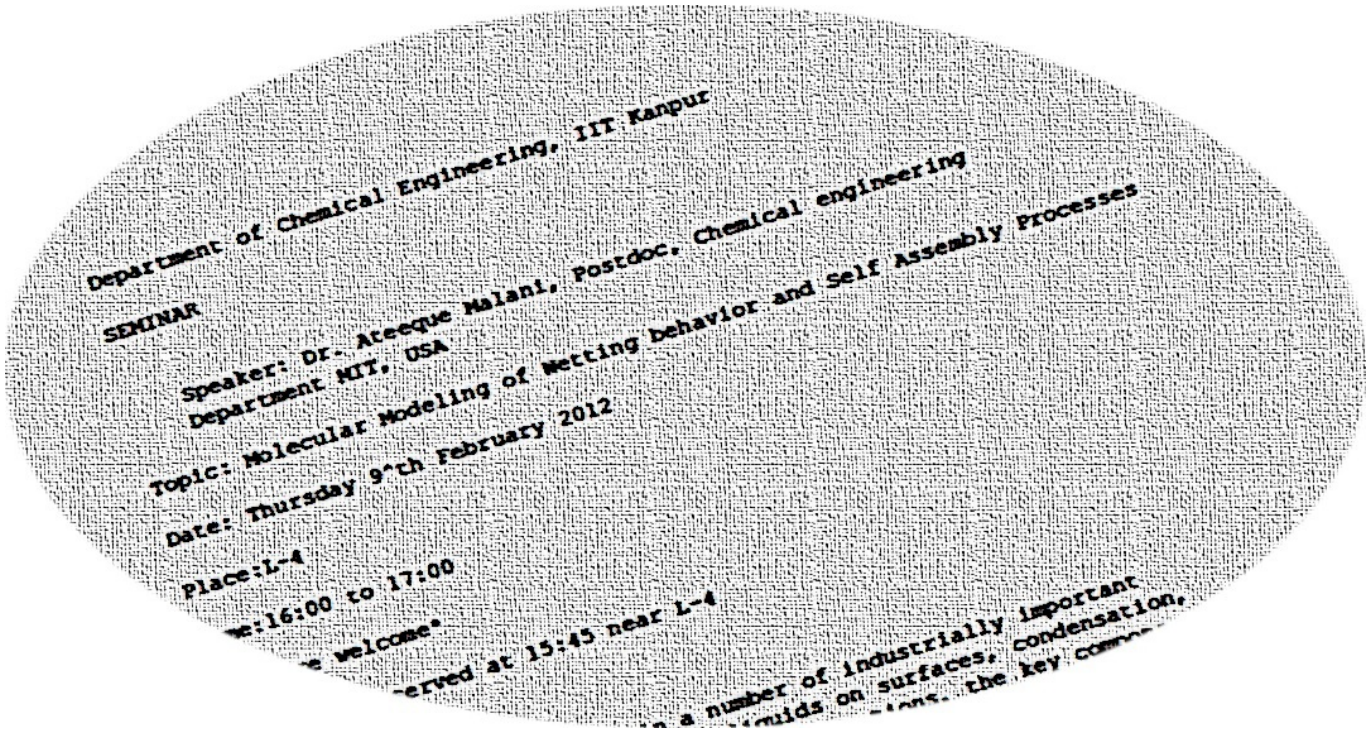

IIT Bombay, January 25, 2017

Molecular modelling of wetting behaviour

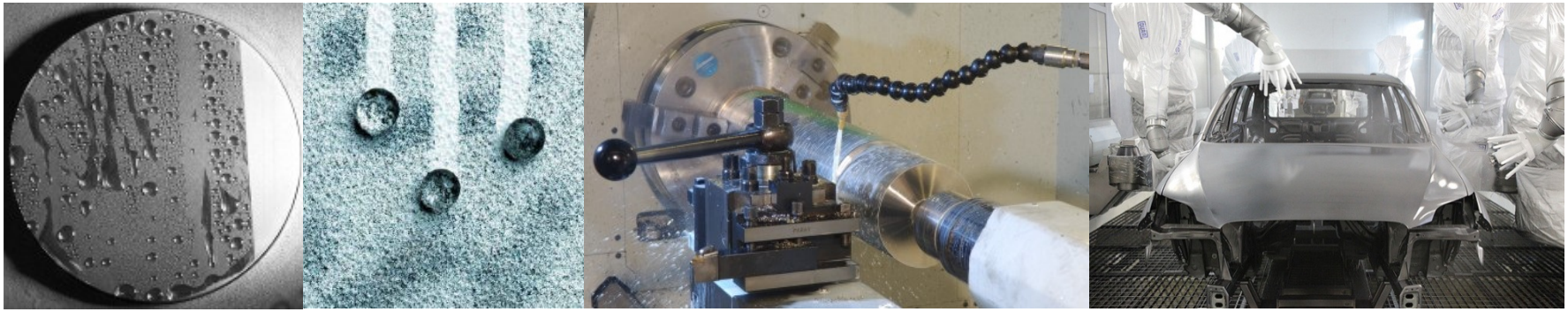

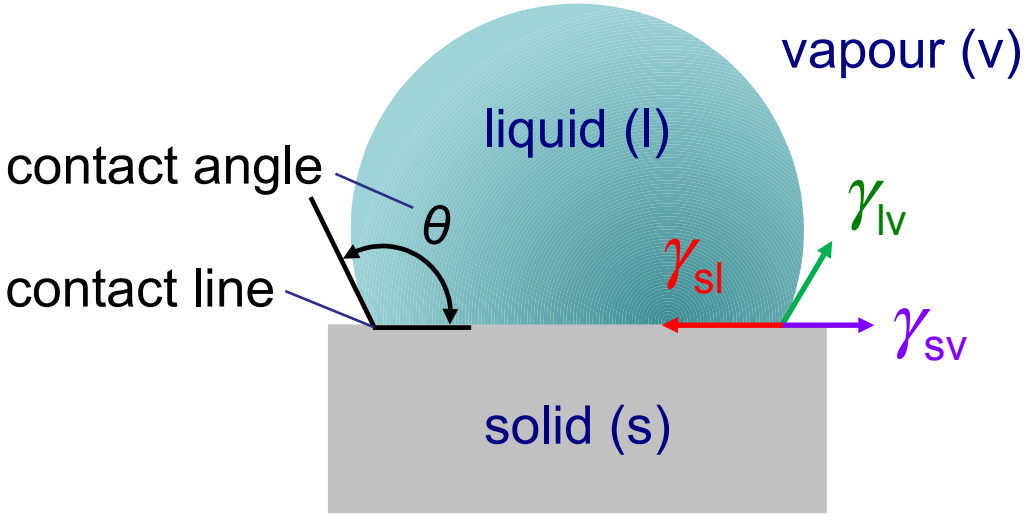

Young equation[1]

$$\cos\theta = \frac{\gamma_{sv} - \gamma_{sl}}{\gamma_{lv}}$$

[1]T. Young, *Phil. Trans. R. Soc. London* 95, 65, **1805**

Computational Molecular Engineering

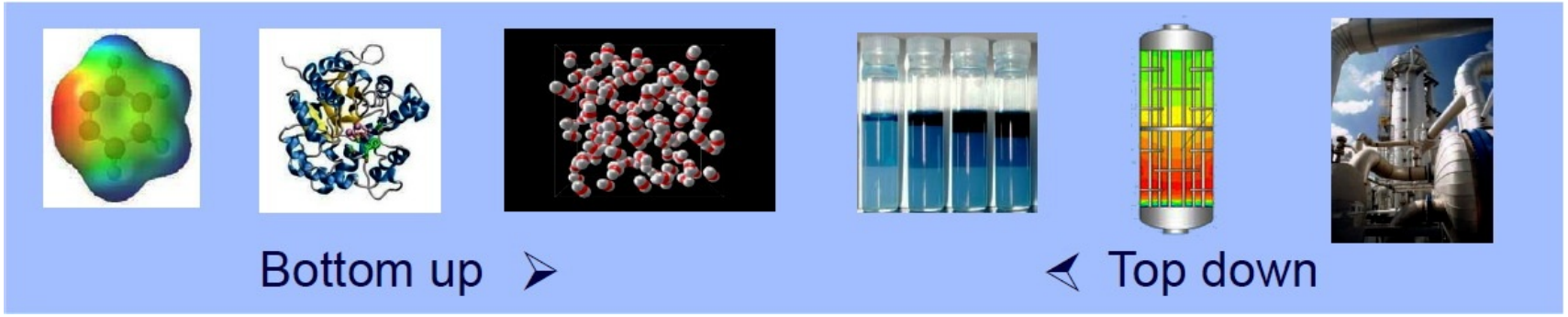

From Physics (qualitative accuracy)

- Physically realistic modelling of intermolecular interactions
- Separate contributions due to repulsive and dispersive as well as electrostatic interactions

To Engineering (quantitative reliability)

- No blind fitting, but parameters of *effective pair potentials* are adjusted to experimental data
- Physical realism facilitates reliable interpolation and extrapolation

Molecular Force Field Methods

Geometry

Rigid bond lengths and angles

Dispersion and repulsion

Lennard-Jones potential:
Size and energy parameters

Electrostatics

Point polarities
(charge, dipole, quadrupole):
Position and magnitude

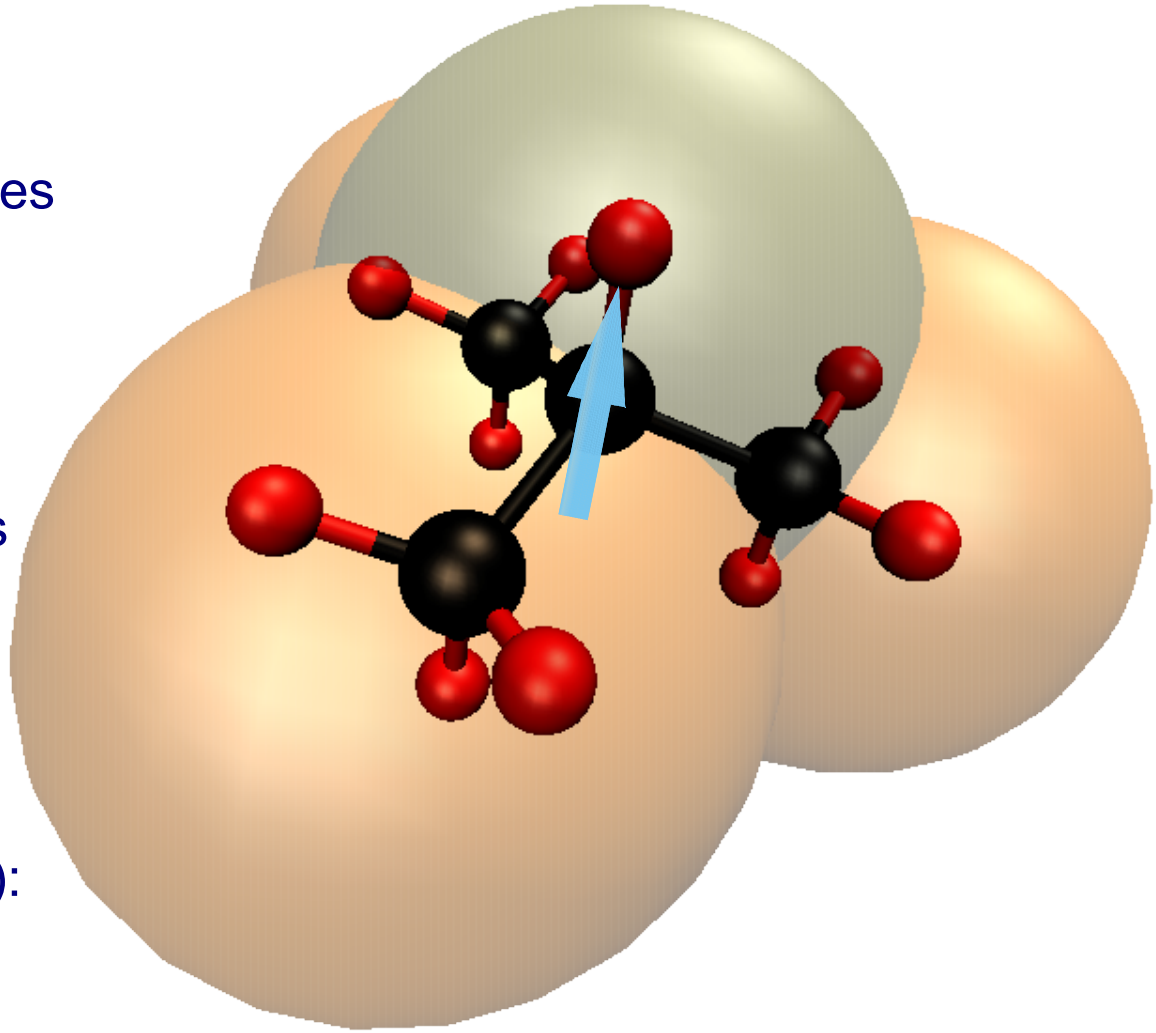

Scalable molecular dynamics simulation

Collaboration within

IMEMO (2008 – 2011)
SkaSim (2013 – 2016)
TaLPas (2017 – 2020)

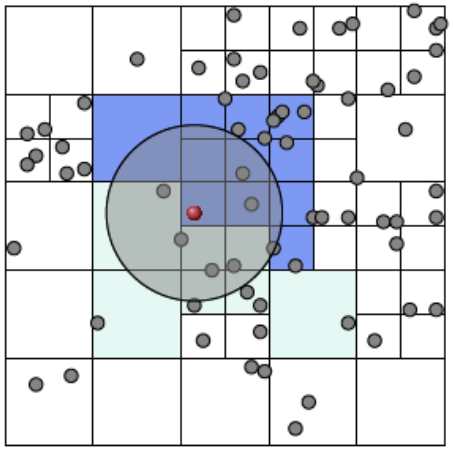

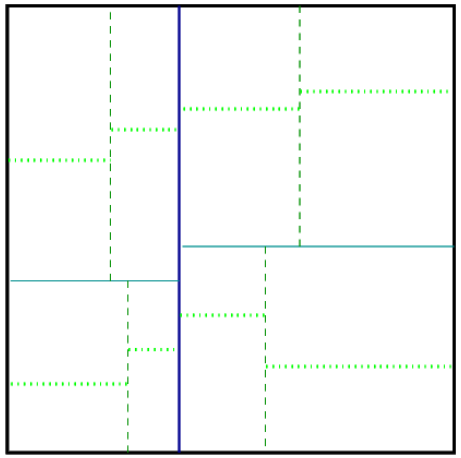

Bundesministerium für Bildung und Forschung

BASF
The Chemical Company

SkaSim

Lehrstuhl für Thermodynamik
Prof. Dr.-Ing. H. Hasse

Technische Universität München

ThEt
UNIVERSITÄT PADERBORN
Die Universität der Informationsgesellschaft

HLRS

Scalable molecular dynamics simulation

Spatial domain decomposition

Dynamic load balancing

Communication (almost) only with neighbour processes

Linked-cell data structure near-field pair potentials

Summation techniques, e.g. Janeček, FMM, for far field

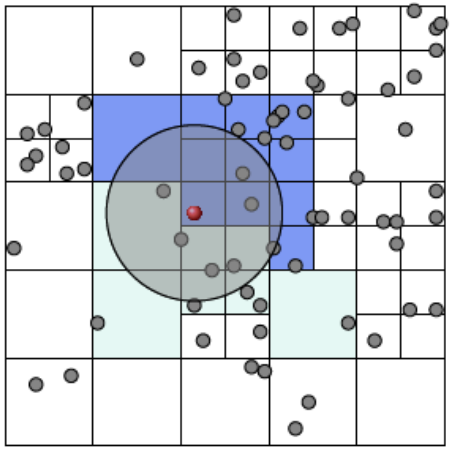

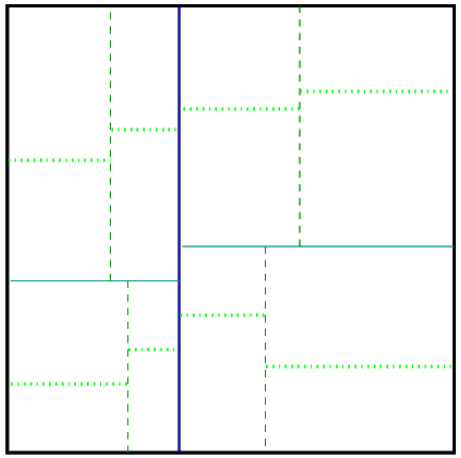

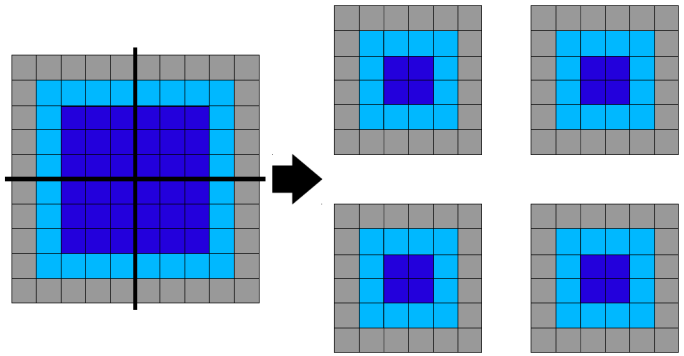

(non-blocking, over-lapping MPI send/ receive operations)

large systems “1”: molecular dynamics

http://www.ls1-mardyn.de/

Scalable molecular dynamics simulation

Scaling of *ls1 mardyn* examined on SuperMUC up to 146 016 cores.

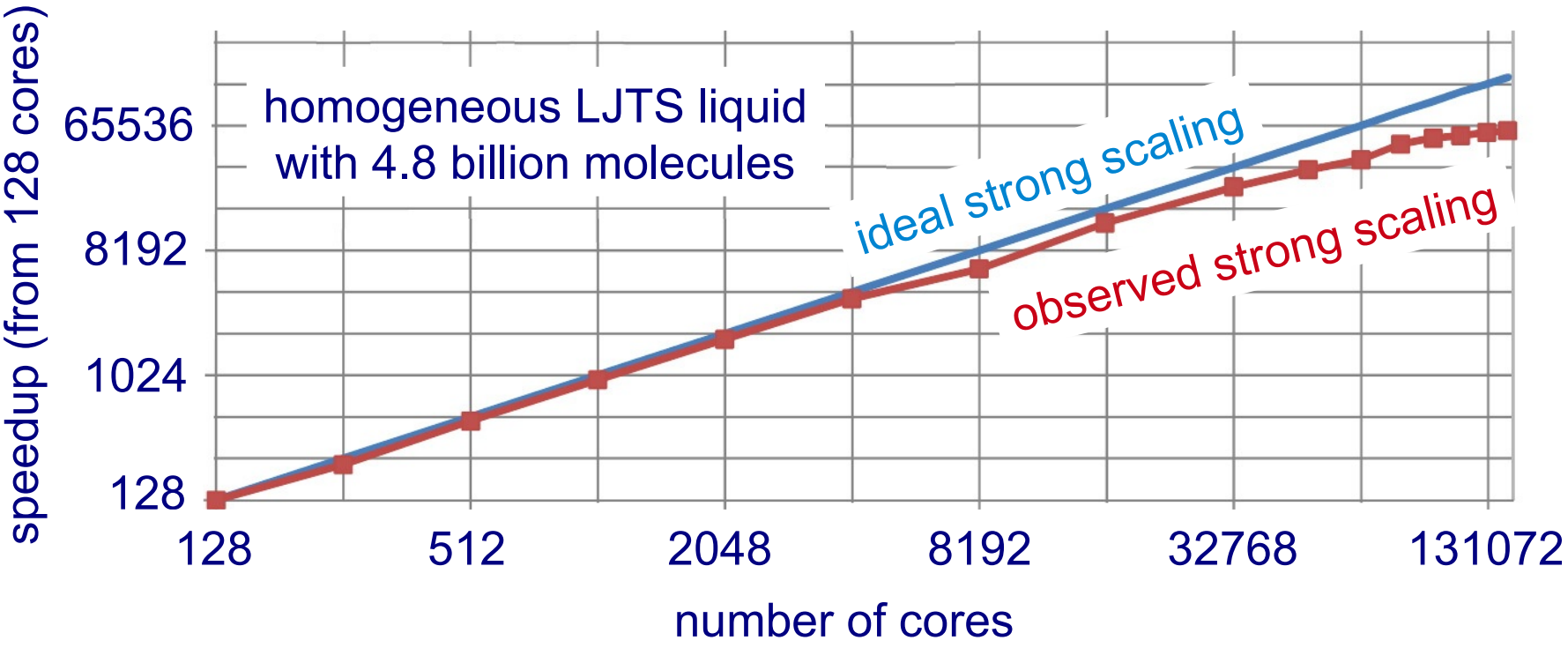

Molecular dynamics world record (2013)

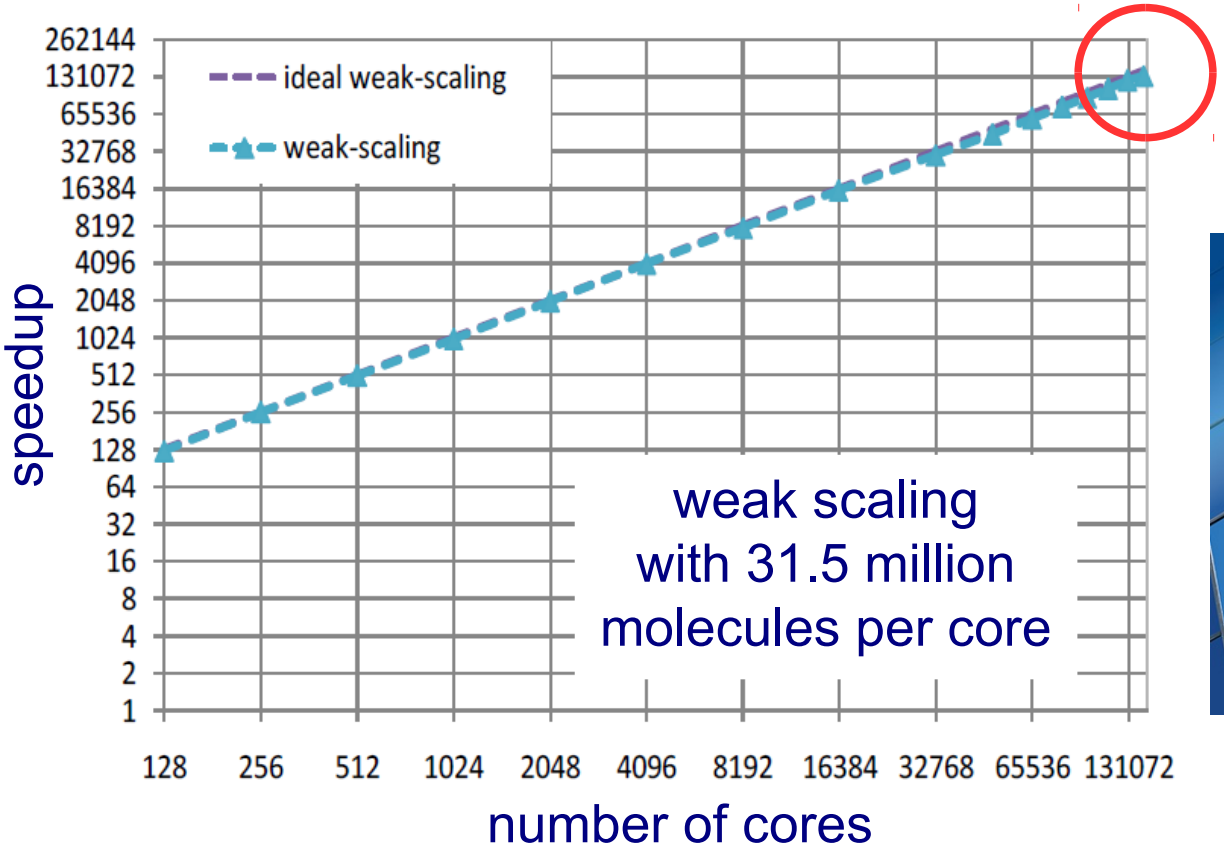

Up to $N = 4 \cdot 10^{12}$ on SuperMUC

MD world record achieved from simulations of a homogeneous LJTS liquid.

MD simulation of heterogeneous systems

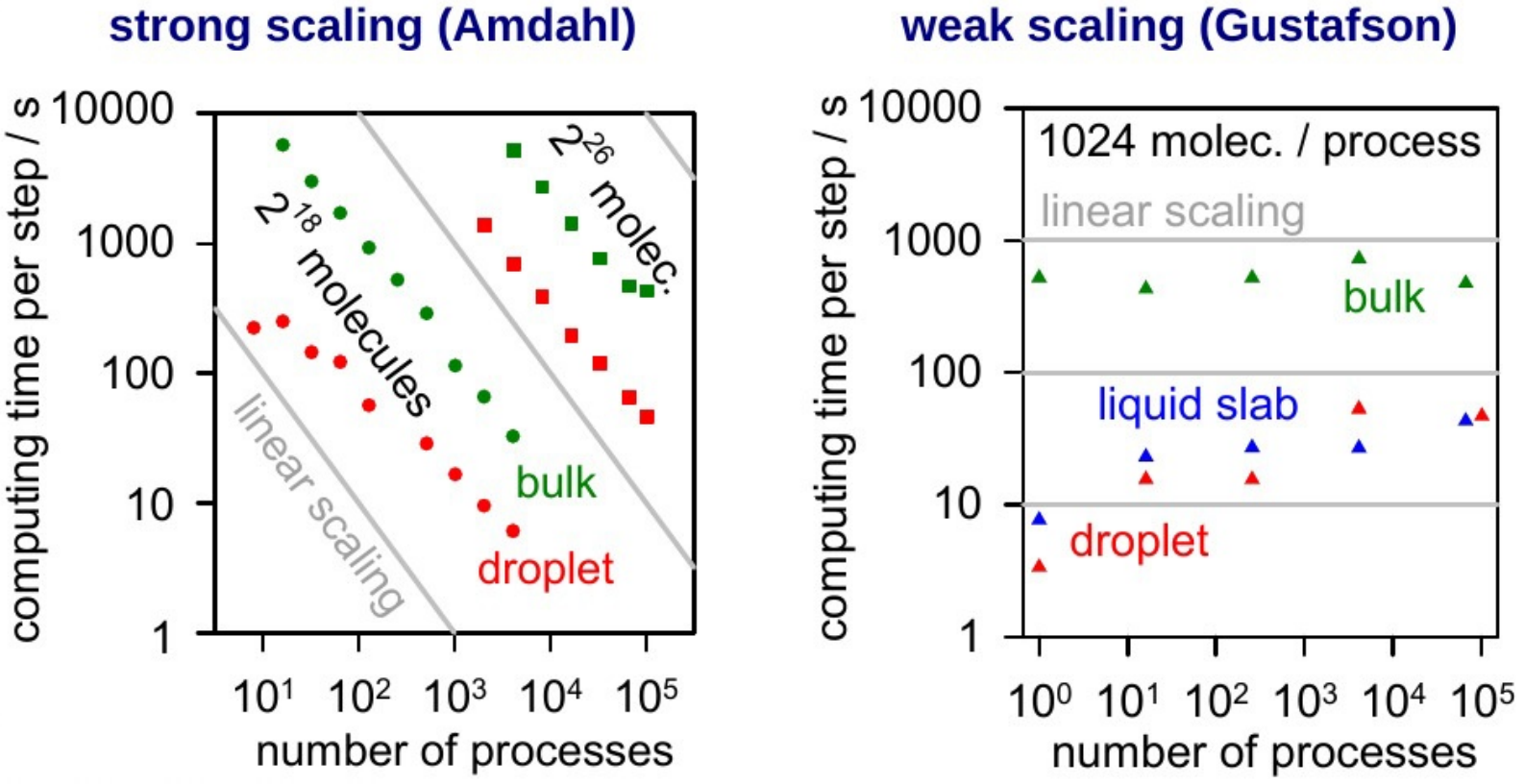

Technically / scientifically relevant simulations of large systems always deal with *heterogeneous* systems (e.g. at vapour-liquid interfaces).

Molecular modelling of wetting behaviour

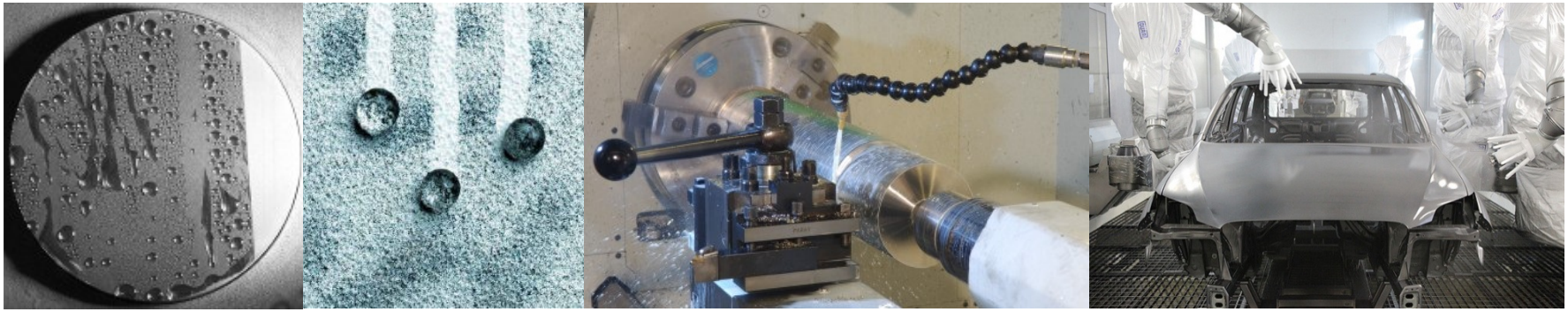

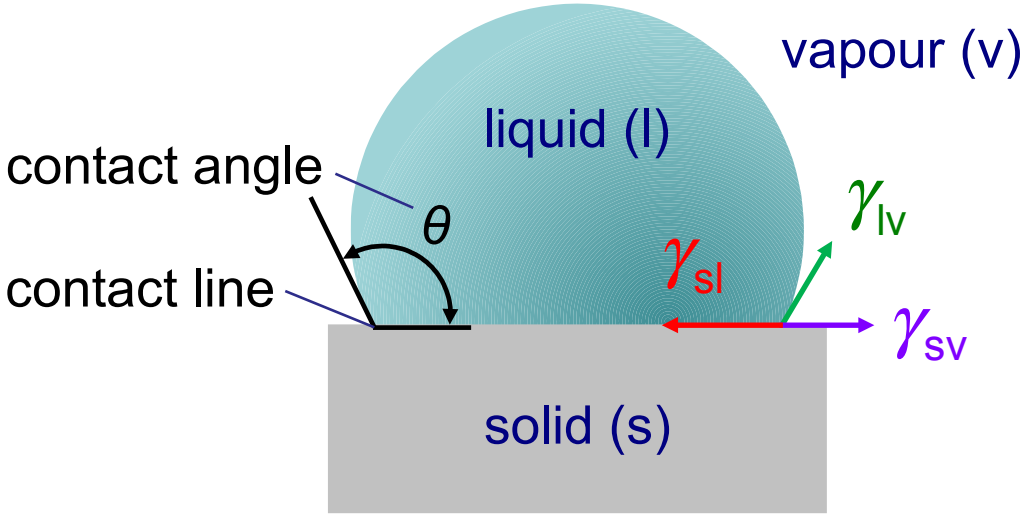

Young equation[1]

$$\cos\theta = \frac{\gamma_{sv} - \gamma_{sl}}{\gamma_{lv}}$$

[1]T. Young, *Phil. Trans. R. Soc. London* 95, 65, **1805**

Contact angle and fluid-solid interaction

LJTS potential for fluid (f) and substrate (s) with $\sigma_{fs} = \sigma_f$ and $\varepsilon_s = 100\ \varepsilon_f$.

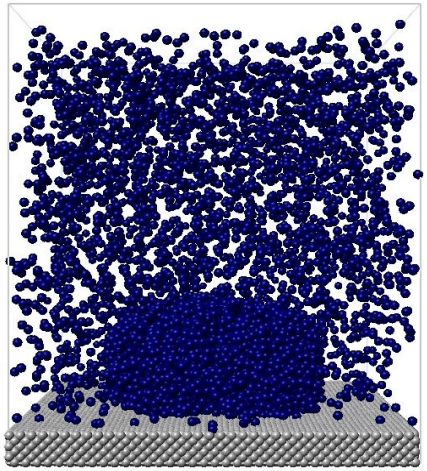

Variation of temperature, dispersion $\zeta = \varepsilon_{fs}/\varepsilon_f$, and density of the substrate.

Contact angle and fluid-solid interaction

LJTS potential for fluid (f) and substrate (s) with $\sigma_{fs} = \sigma_f$ and $\varepsilon_s = 100\ \varepsilon_f$.

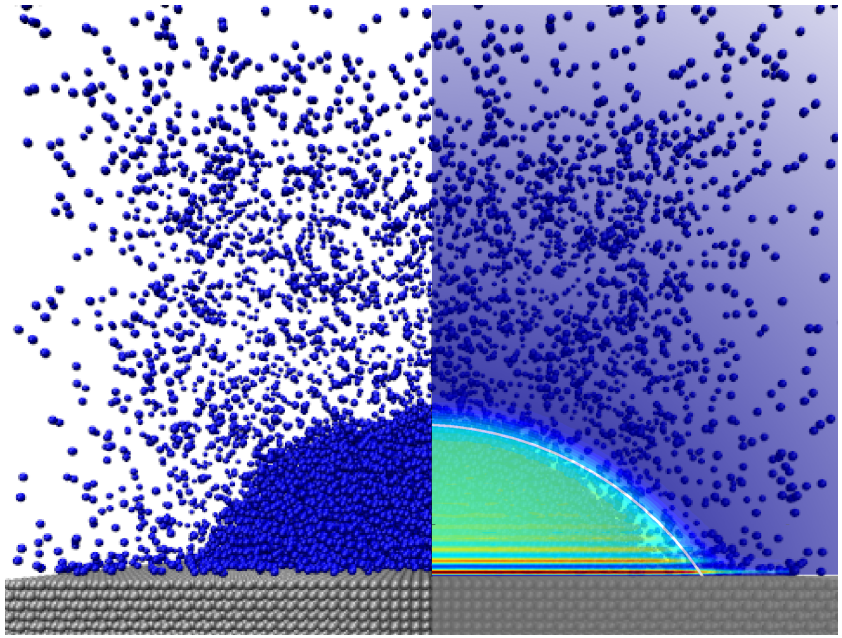

S. Becker *et al.*, *Langmuir* 30, 13606, **2014**

Correlation of the density profile by

$$\rho(r, y) = f(r) \cdot [h(y) + 1],$$

with the exponential decay term $h(y)$

and a hyperbolic tangent profile $f(r)$.

The fluid-solid contact angle is determined at the intersection of the solid surface with the vapour-liquid interface given by the correlation expression.

Influence of the droplet size

Combination of multiple finite-size effects: $\cos\theta = \frac{1}{\gamma_{vl}}\left(\gamma_{vs} - \gamma_{ls} - \frac{\tau}{R_{lin}}\right)$

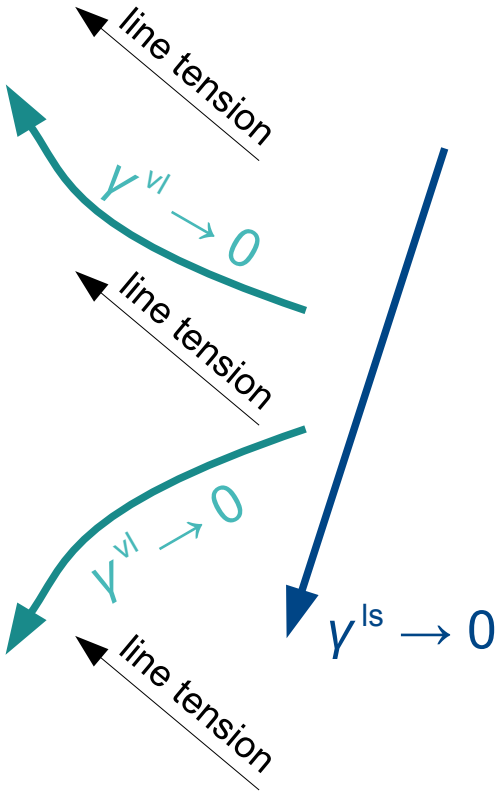

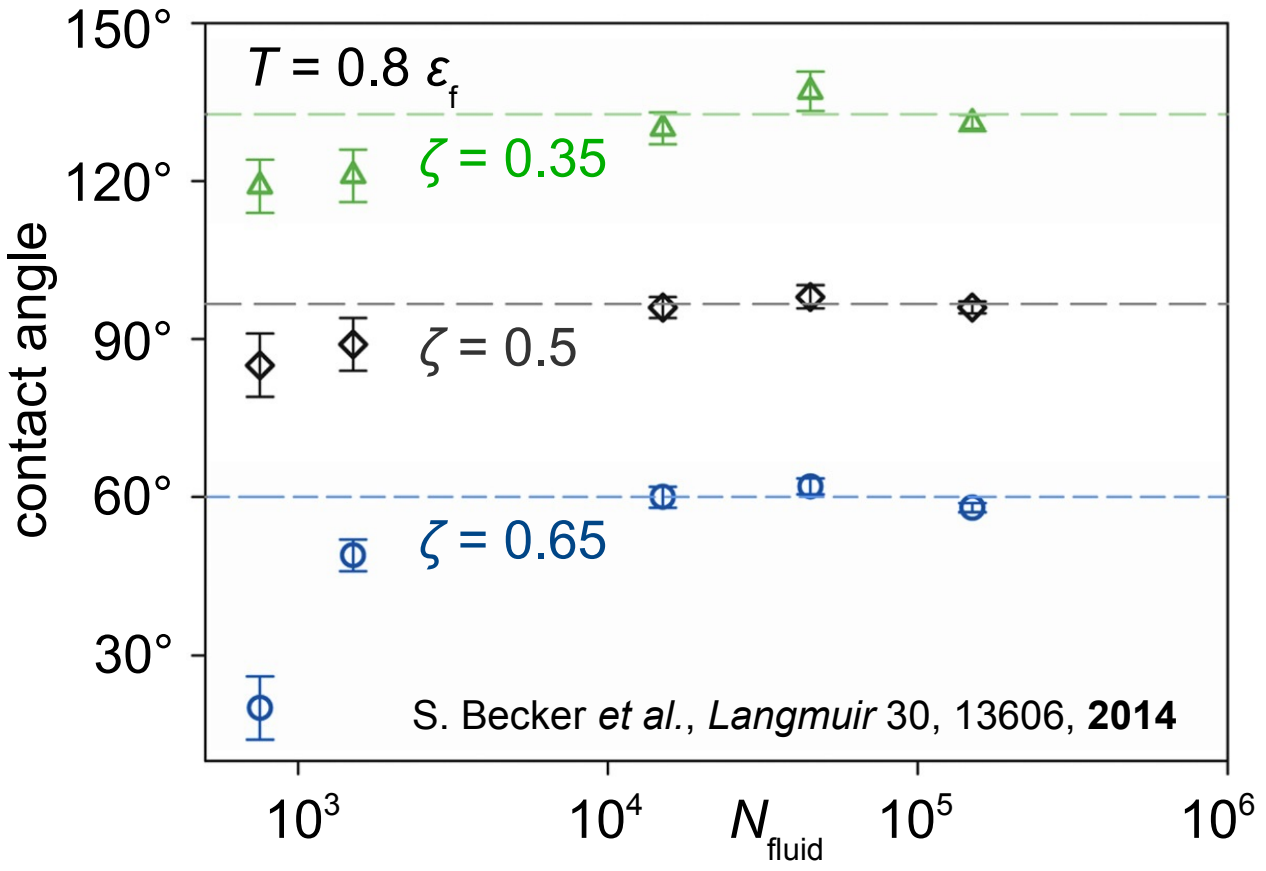

Contact angle and fluid-wall interaction

Variation of the reduced fluid-wall dispersion energy ζ, at constant T:

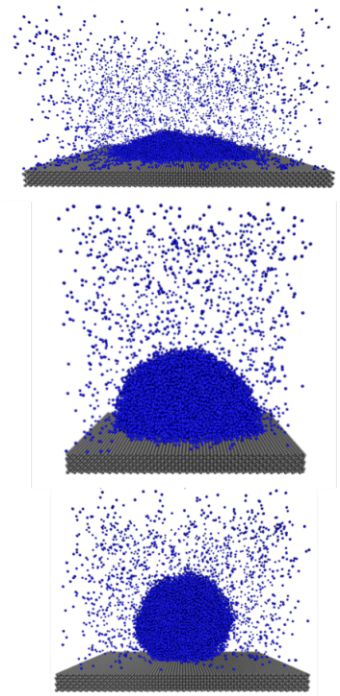

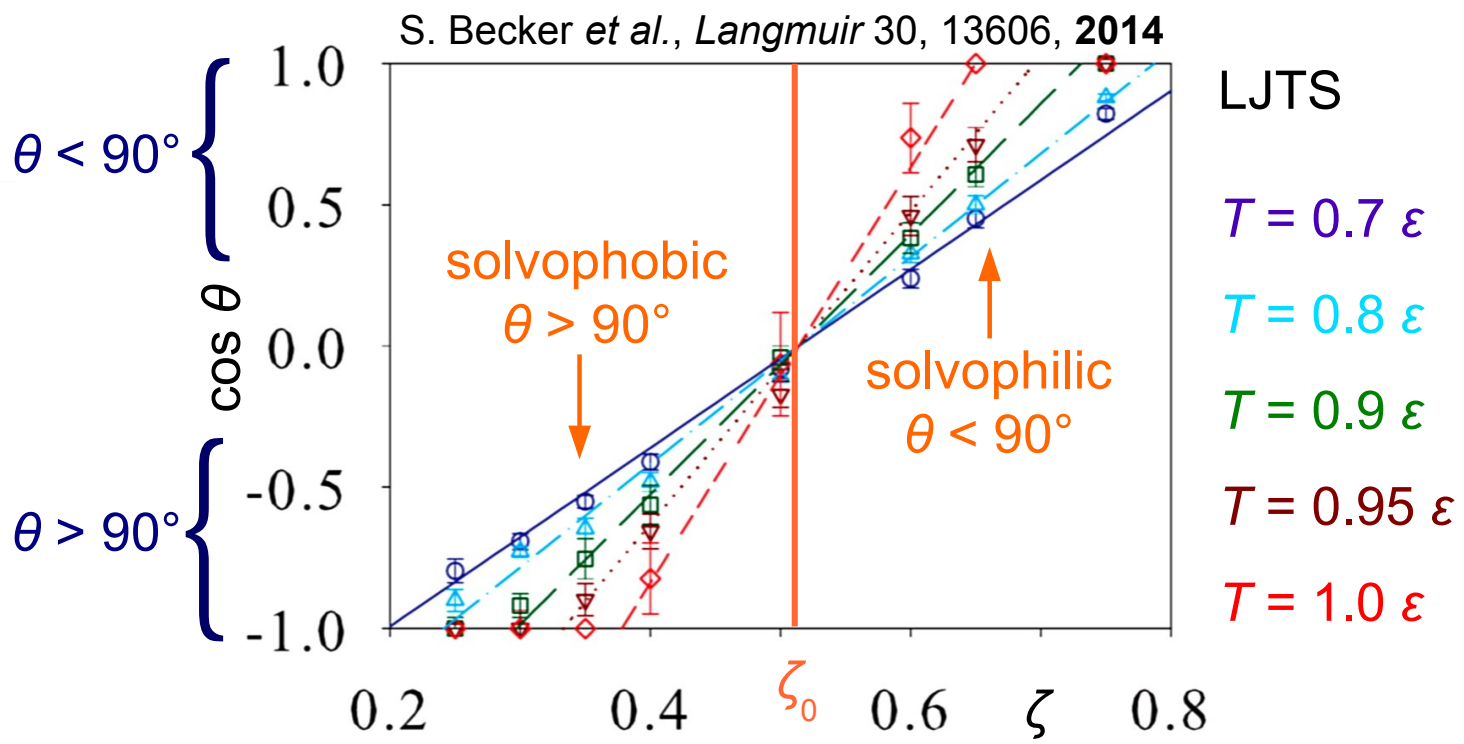

Correlation: cos θ proportional to $\zeta - \zeta_0$ for $\zeta_0 = 0.52$ at all temperatures.

Characterization for dispersive interaction

The substrate model and the unlike interaction determine the well depth *W*.

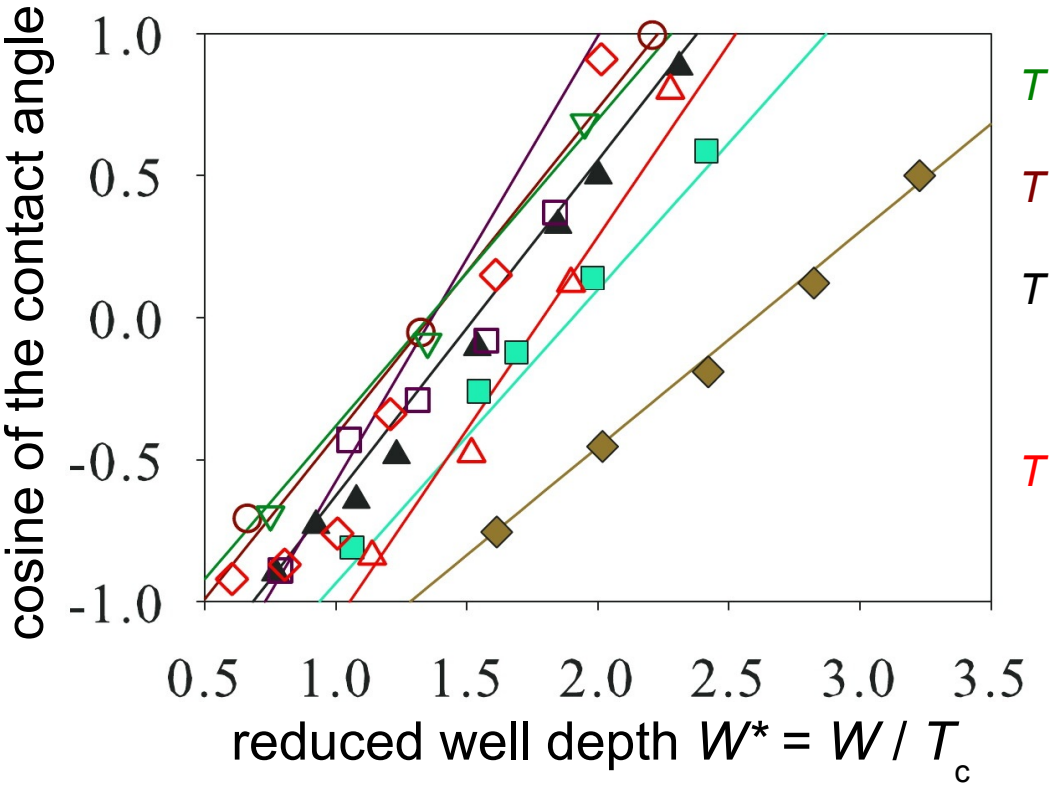

T = 0.7 *ε*, Grzelak *et al.* (2010)

T = 0.75 *ε*, Ingebrigtsen and Toxværd (2007)

T = 0.8 *ε*, present work[1] (▲) with $\sigma_s = \sigma$,
(■) with $\sigma_s = 0.8\ \sigma$, (♦) with $\sigma_s = 0.64\ \sigma$

T = 0.9 *ε*, (Δ) Nijmeijer *et al.* (1990),
(◊) Nijmeijer *et al.* (1992),
and (□) Tang and Harris (1995)

[1]S. Becker *et al.*, *Langmuir* 30(45), 13606–13614, **2014**

Lines: General correlation $\theta(T^*, W^*, \rho)$ for contact angles of LJ systems.

Fluid-solid interaction and boundary slip

$\varepsilon_{fw} = 0.05\ \varepsilon_f$

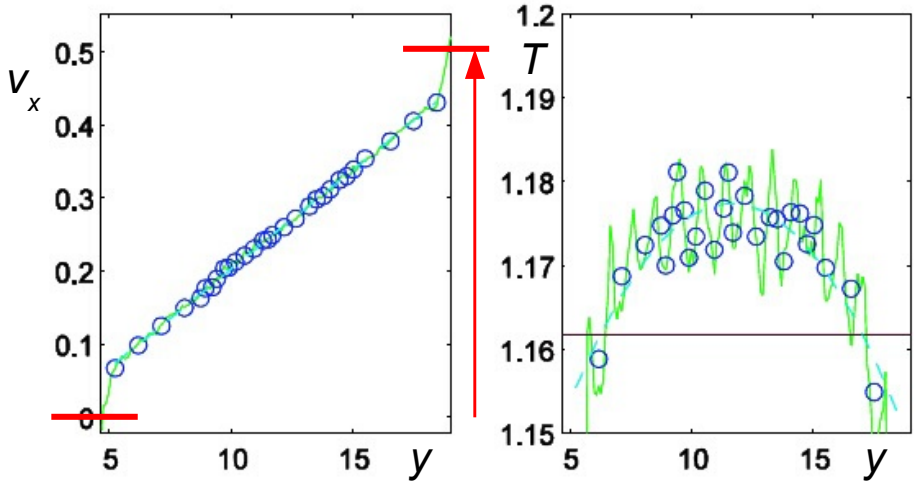

$\varepsilon_{fw} = 0.5\ \varepsilon_f$

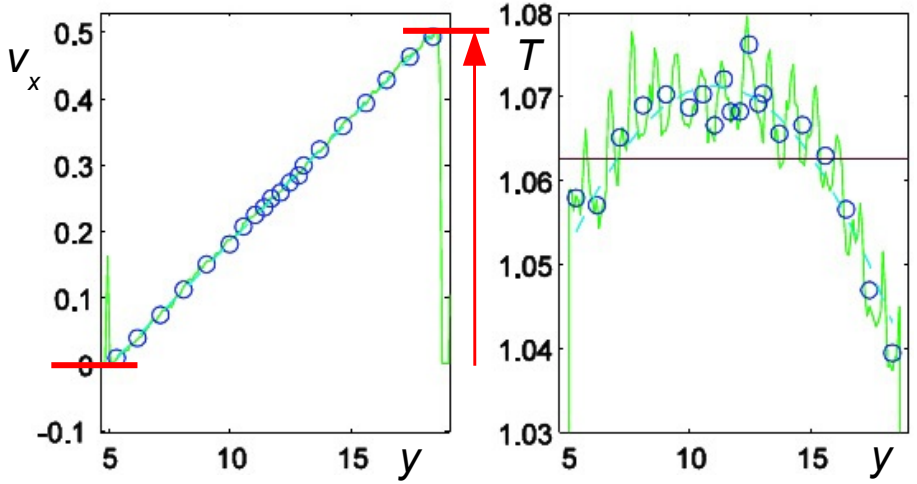

Scenario: Fluid and solid LJTS with $\varepsilon_w = 100\ \varepsilon_f$ and $\sigma_w = \sigma_f$

$$T_w = 0.8\ \varepsilon_f$$
$$\Delta y_w = 15\ \sigma_f$$
$$\Delta v_w = 0.5\ (\varepsilon_f / m_f)^{1/2}$$

Fluids **attracted more strongly** to the walls support greater shear rates **without boundary slip**. A stronger unlike interaction between the fluid and the wall **improves heat transfer** from the fluid to the wall.

Nanoindentation and nanoscratching

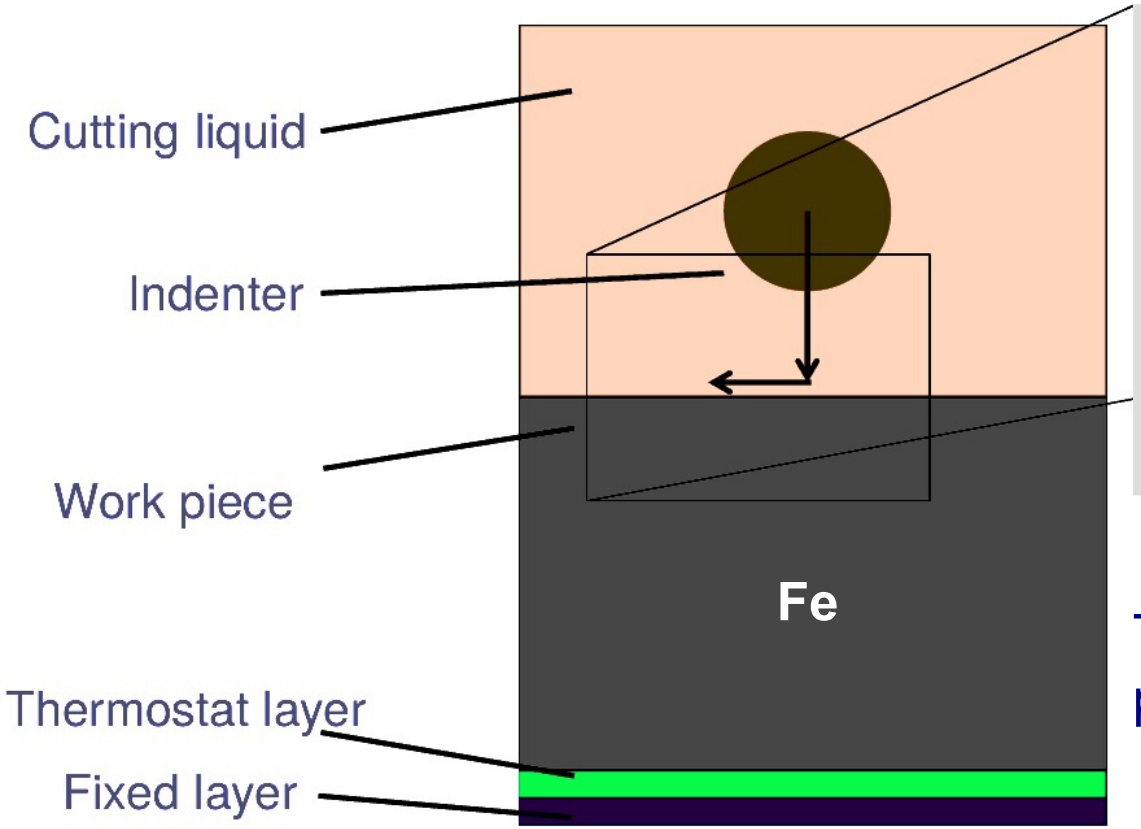

Fluid and fluid-solid: LJTS

Fluid-solid: $\zeta = 0.5$

Iron: Mendelev potential[1]

Indenter: Rigid cylinder (with LJTS sites)

Thermostat acting on remote part of the work piece,

$$T_{ext} = 0.8\ \varepsilon_f,$$

fluid density $\rho_f = 0.8\ \sigma^{-3}$.

[1]M. Mendelev, S. Han, D. Srolovitz, G. Ackland, D. Sun, M. Asta, *Philos. Mag.* 83, 3977, **2003**.

Fluid behaviour during nanoscratching

MD simulation of indentation and scratching with different orders of magnitude for the fluid-solid interaction.

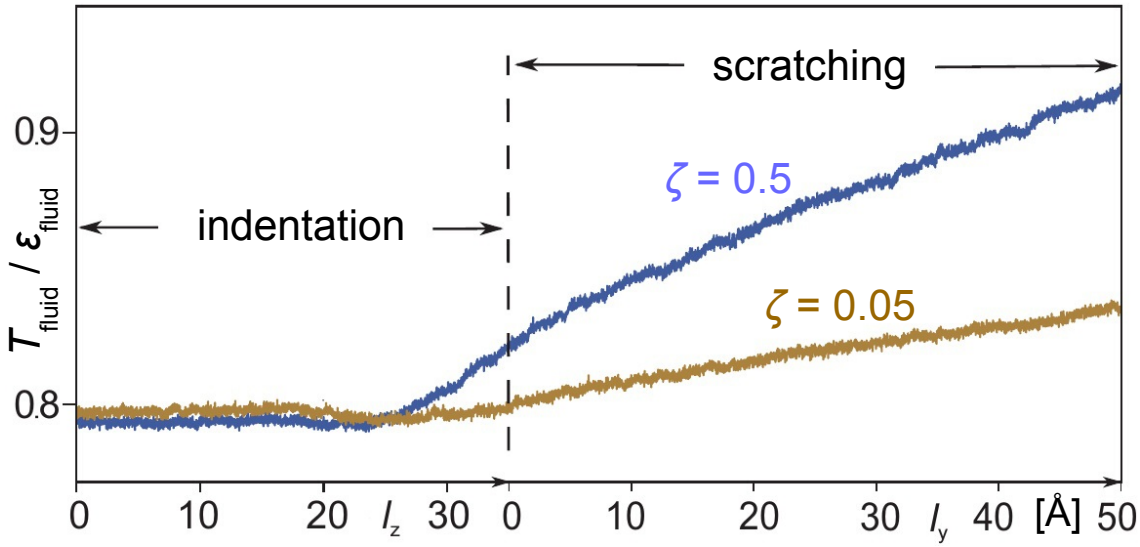

temperature profile (ζ = 0.5)

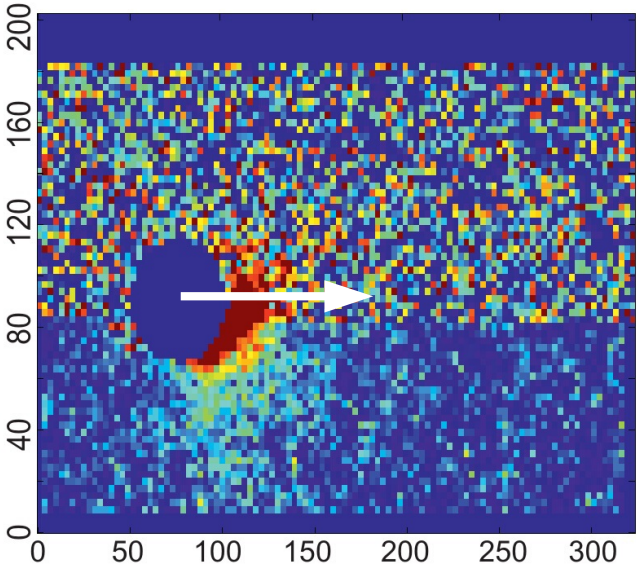

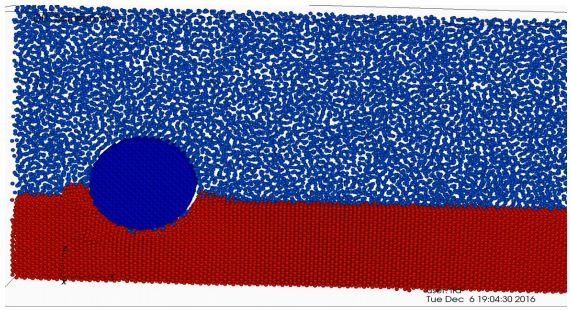

Heat transfer from work piece to liquid

MD simulation of indentation and scratching with different orders of magnitude for the fluid-solid interaction.

temperature profile ($\zeta = 0.5$)

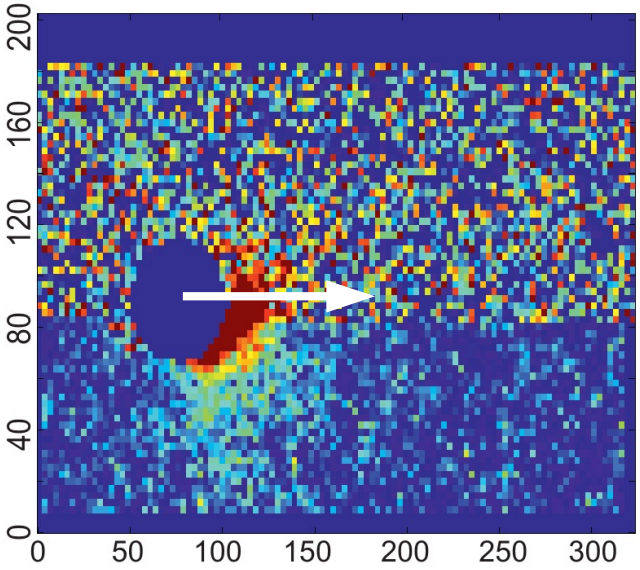

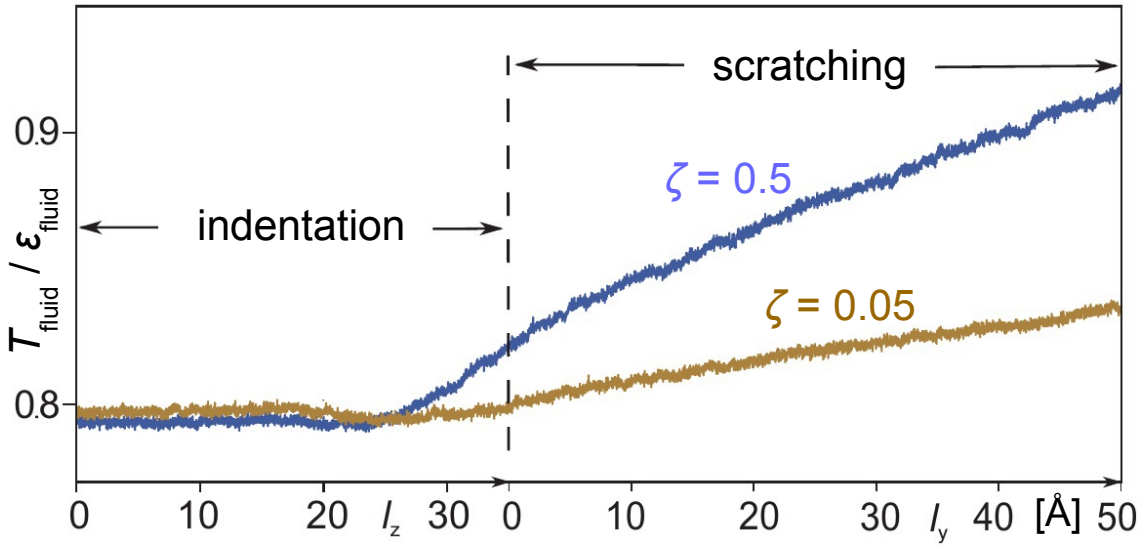

Greater fluid-wall dispersion

- reduces Kapitza (thermal) resistance
  here, by 10 to 50%, depending on T
- increases friction (LJ is not a lubricant)
  here, F_T/F_N increased by 20 to 30%

Morphology of the substrate surface

"Morphological analysis is simply an ordered way of looking at things." [1]

[1] F. Zwicky, *The Observatory* 68, 121, **1948**

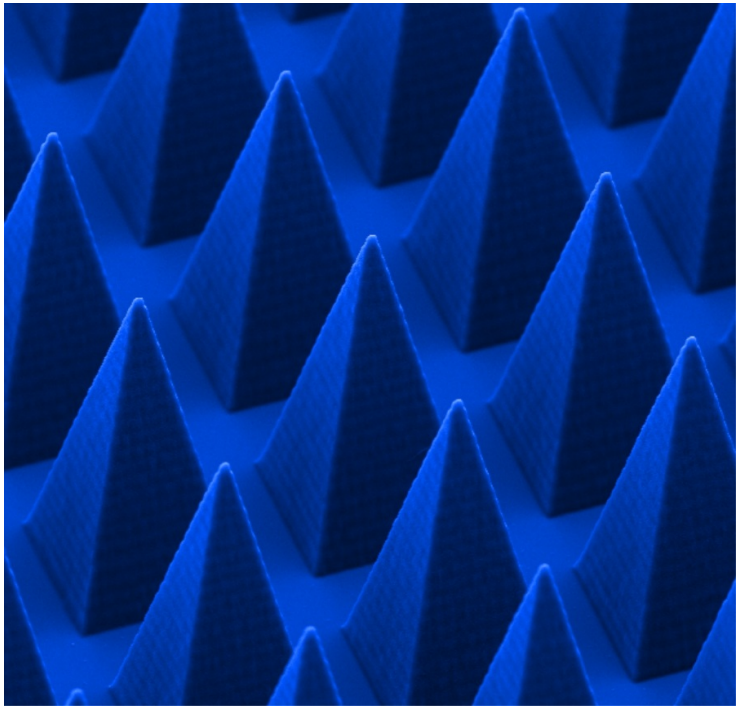

(source: Optics group, U. of Kaiserslautern)

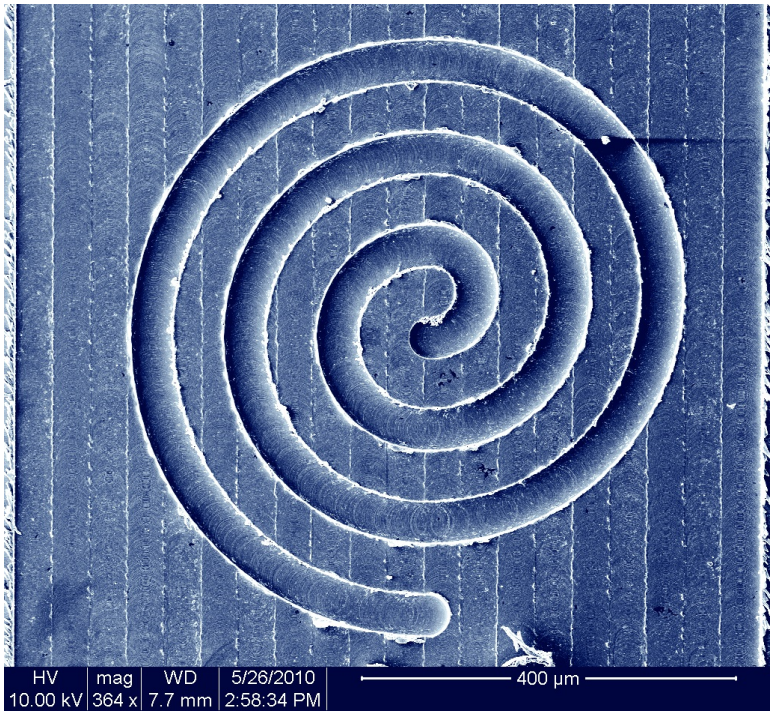

(source: FBK group, U. of Kaiserslautern)

From planar to structured surfaces

Investigation of the contact angle for a variety of surface morphologies:

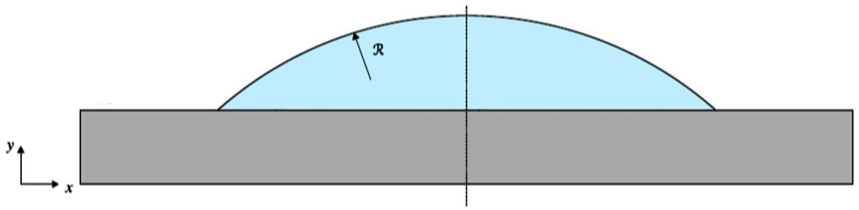

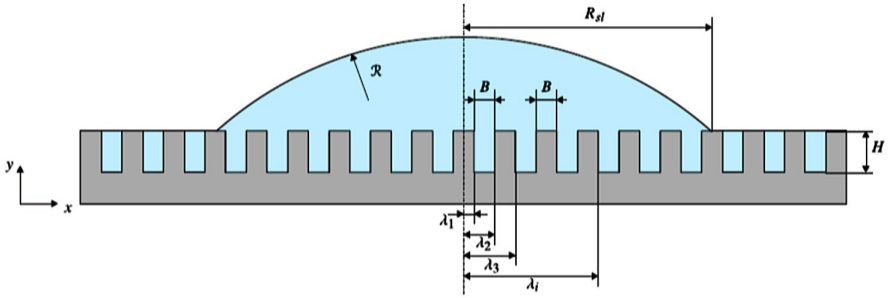

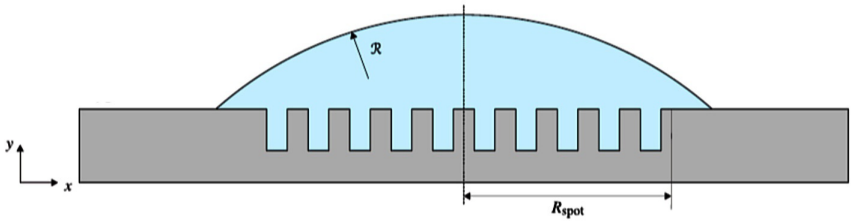

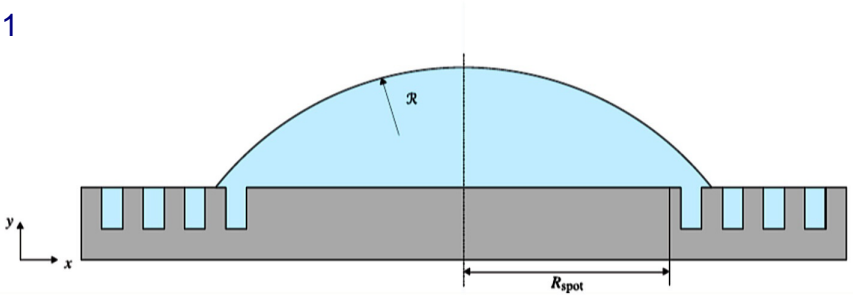

The dependence $\theta_0(T, W, \rho_s)$ is known.[1]

[1] S. Becker *et al.*, *Langmuir* 30, 13606, **2014**

Cassie and Wenzel models

Surface structure is reduced to characteristic ratios of surface areas:[1, 2]

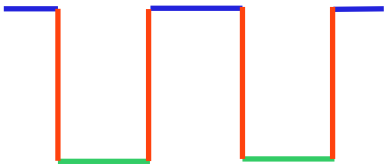

f_1 = unstructured area (“top”)

f_2 = structured area (“bottom”)

f_3 = excess surface area (“side”)

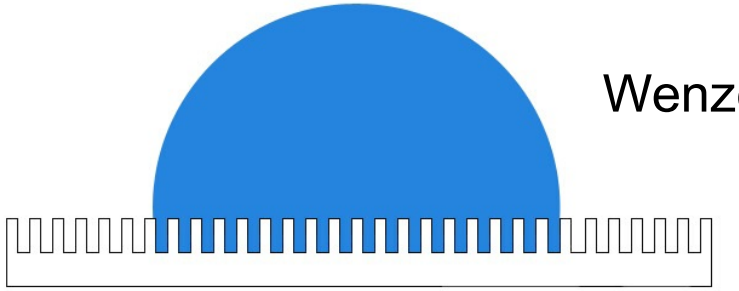

Wenzel roughness factor $w = \frac{f_1+f_2+f_3}{f_1+f_2}$

unstructured fraction $\phi = \frac{f_1}{f_1+f_2}$

The quantities *w* and *φ* describe **average** surface properties.

[1]R. N. Wenzel, *Ind. Eng. Chem.* 28, 988, **1936**, [2]A. Cassie, S. Baxter, *Transact. Faraday Soc.* 40, 546, **1944**

Cassie model and impregnation

Cassie[1]

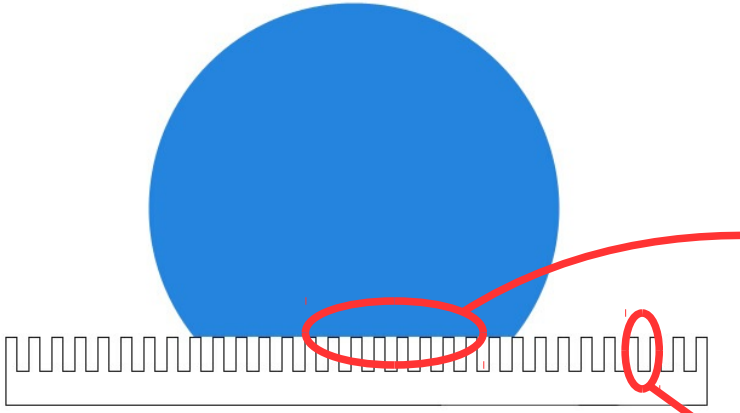

$\gamma_{vv} = 0$

unstructured fraction $\phi = \frac{f_1}{f_1 + f_2}$

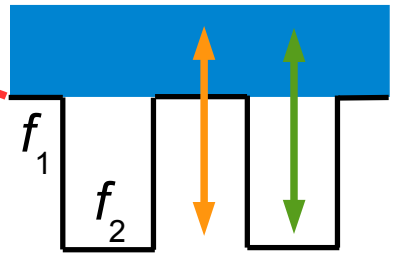

$\varphi\gamma_{ls} + (1 - \varphi)\gamma_{vl}$

Wenzel

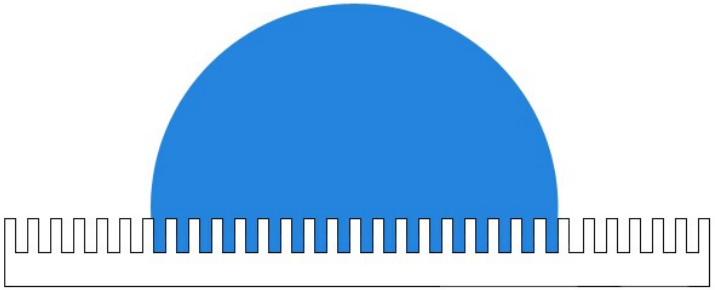

Impregnation[1]

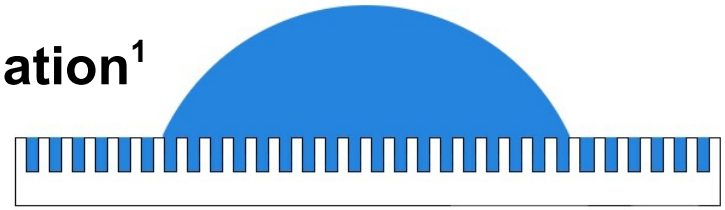

$$|\cos\theta| = |\cos\theta_0| + 1 - \phi$$

[1]A. Cassie, S. Baxter, *Transact. Faraday Soc.* **40** (1944) 546.

Contact angle on an impregnated surface

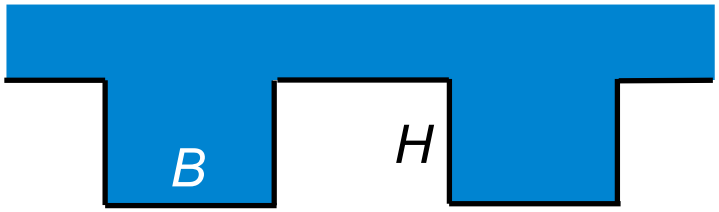

$H = 4.7\ \sigma_f$

$B = 6\ \sigma_f$

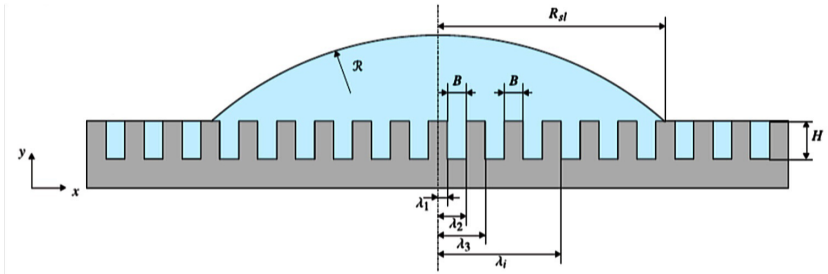

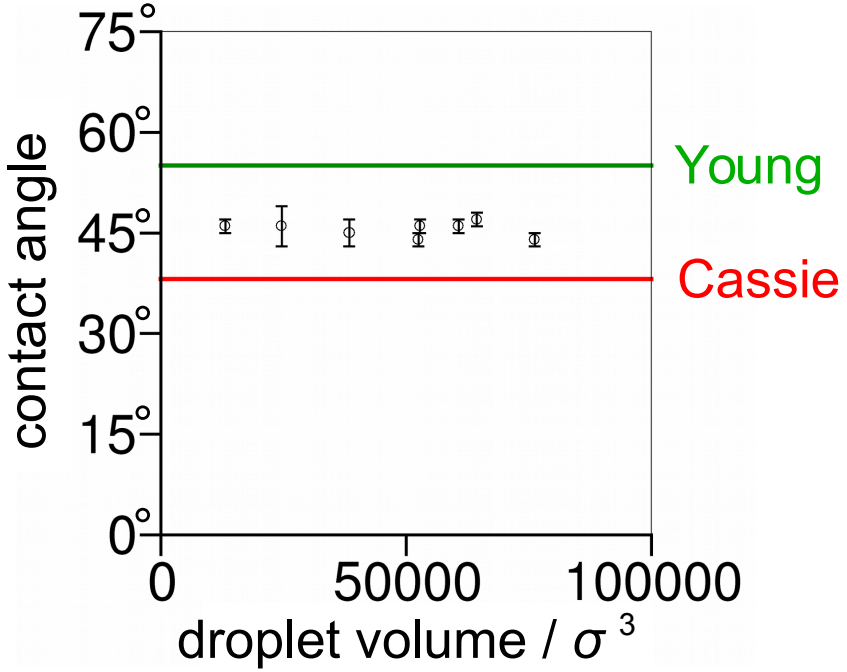

Young contact angle: $\theta_0 = 55°$

Wenzel roughness factor: $w = 1.78$

Unstructured fraction: $\varphi = 0.5$

Wenzel model: $\theta = 0°$

Cassie model: $\theta = 38°$

Contact angle on an impregnated surface

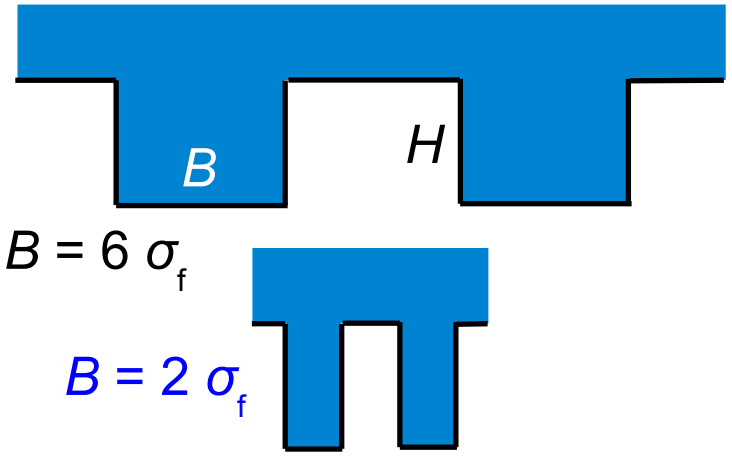

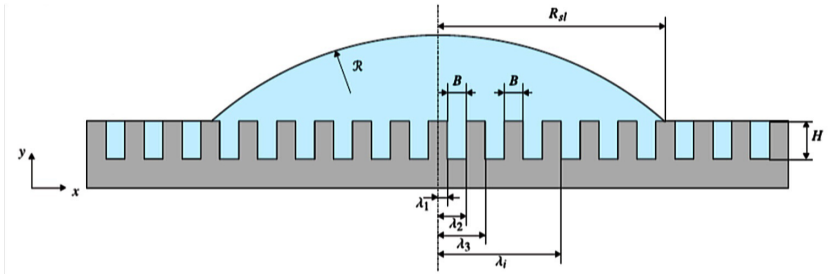

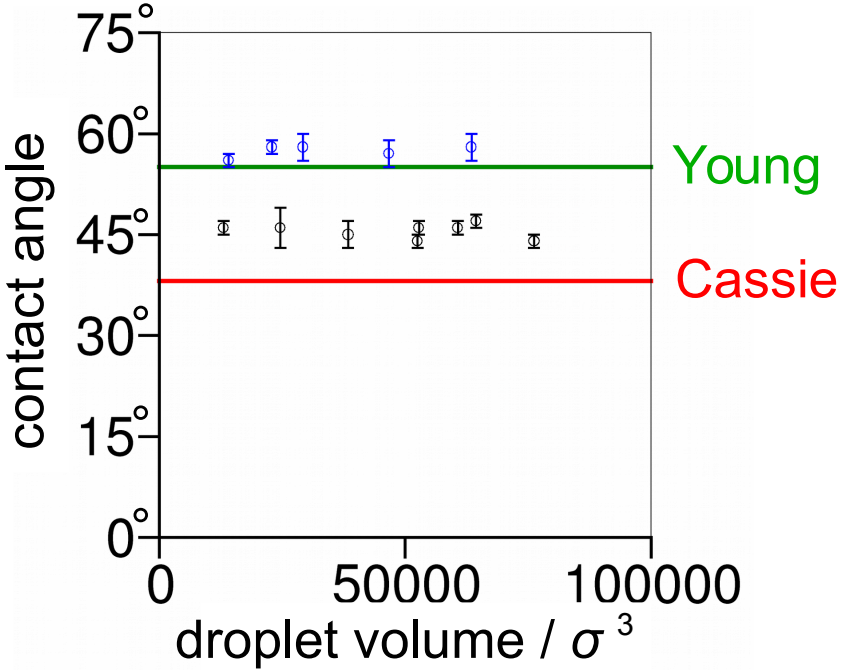

Young contact angle: $\theta_0 = 55°$

Wenzel roughness factor: $w = 1.78, 3.35$

Unstructured fraction: $\varphi = 0.5$

Wenzel model: $\theta = 0°$

Cassie model: $\theta = 38°$

Heterogeneously structured surfaces

Contact angles on the impregnated *homogeneously structured* surfaces:

$\theta = 45°$ for $B = 6\ \sigma_f$ and $\theta = 58°$ for $B = 2\ \sigma_f$.

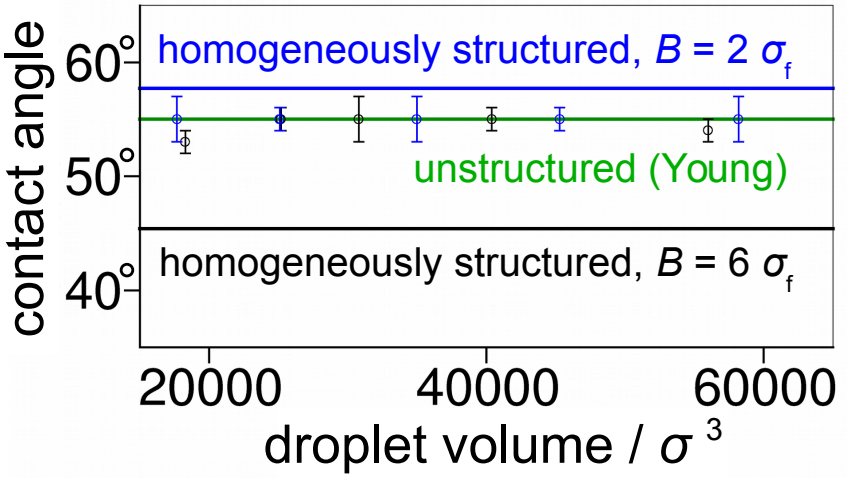

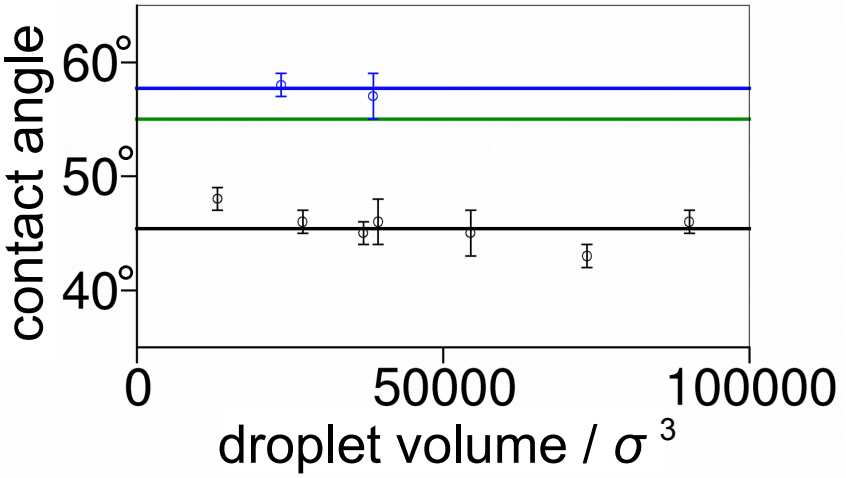

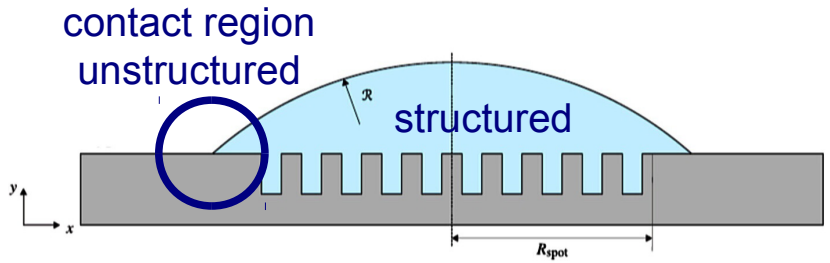

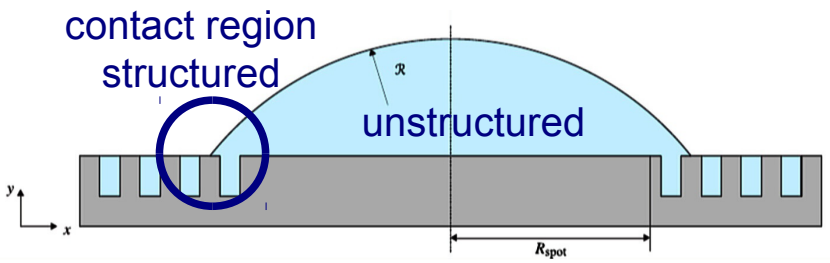

Asymmetrical droplet contours

A symmetry break can be imposed by the boundary conditions, even if the structures themselves have a strictly cylindrical outline.

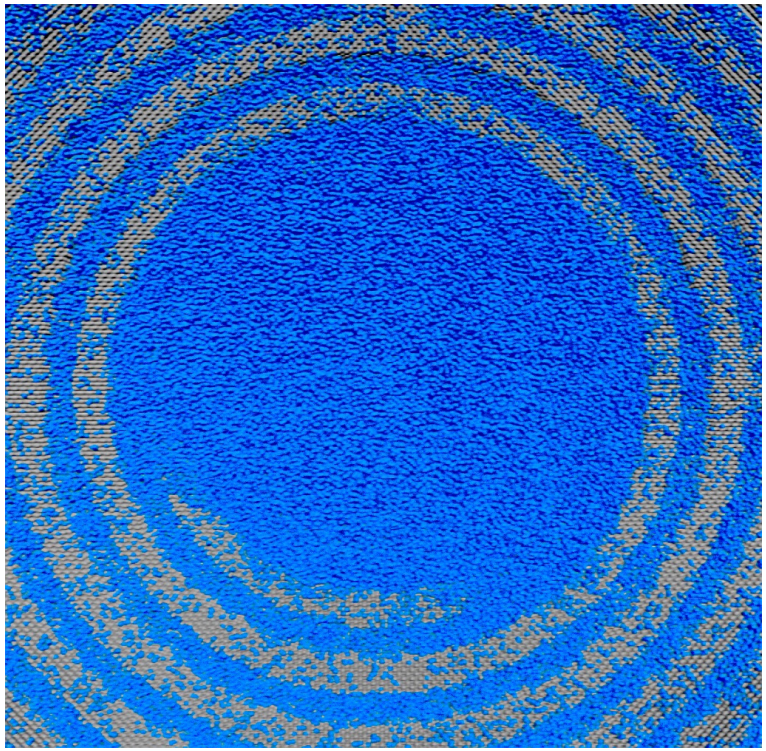

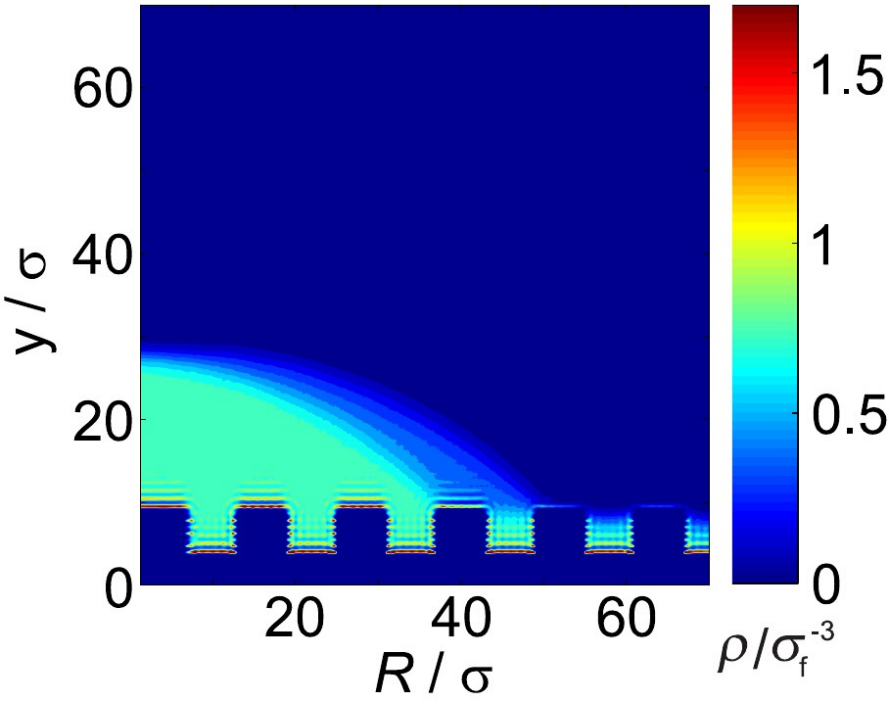

From structured to functionalized surfaces

Protective coating

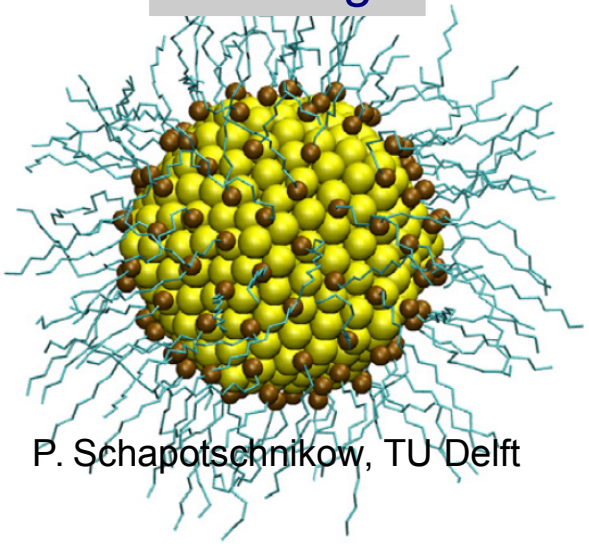

P. Schapotschnikow, TU Delft

superhydrophobic surfaces

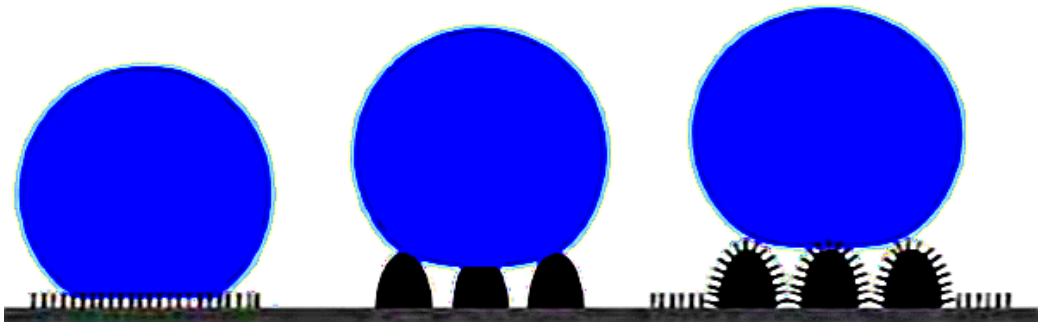

Surface structure influence on pinning

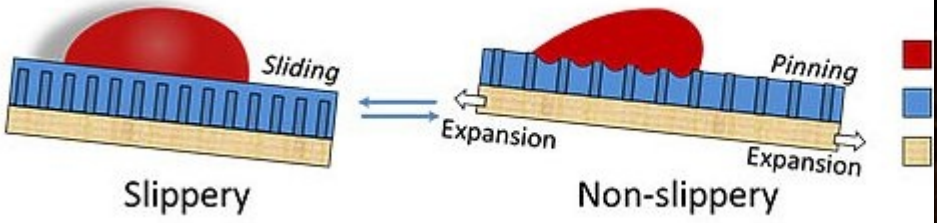

T.-S. Wong, Penn State

Silane self-assembled monolayers on silica

- Super-slip flow of polystyrene on dodecyltrichlorosilane (DTS) monolayer
- Complex surface structure emerging from synthesis by self assembly
- Experiments (here, electron density profiles) yield incomplete information

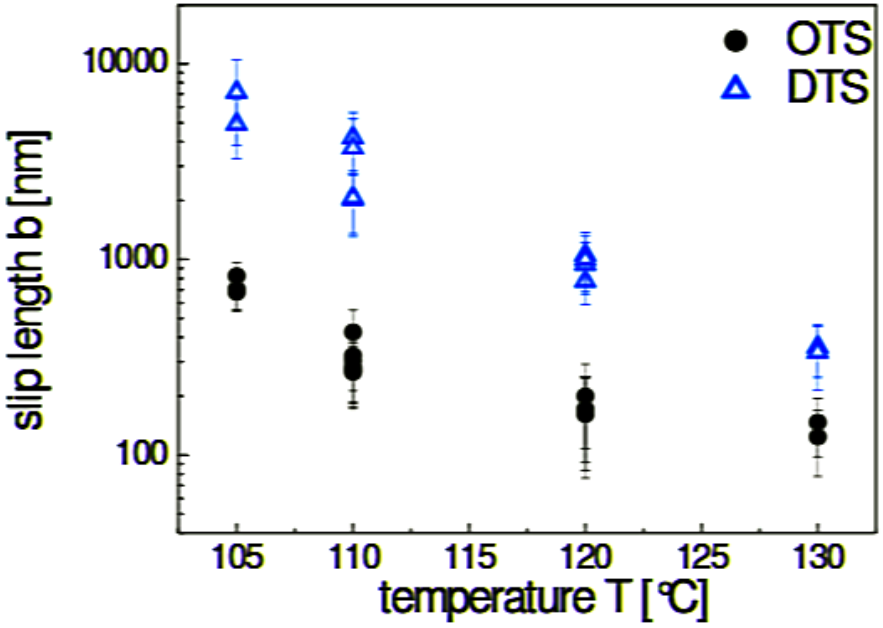

Fetzer *et al.*, Saarland University, **2006**

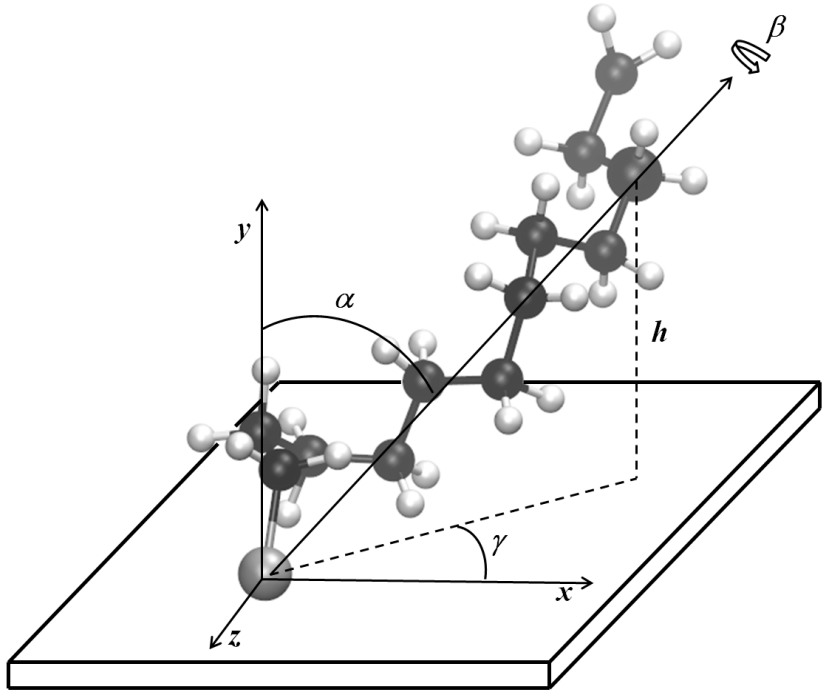

Silane self-assembled monolayers on silica

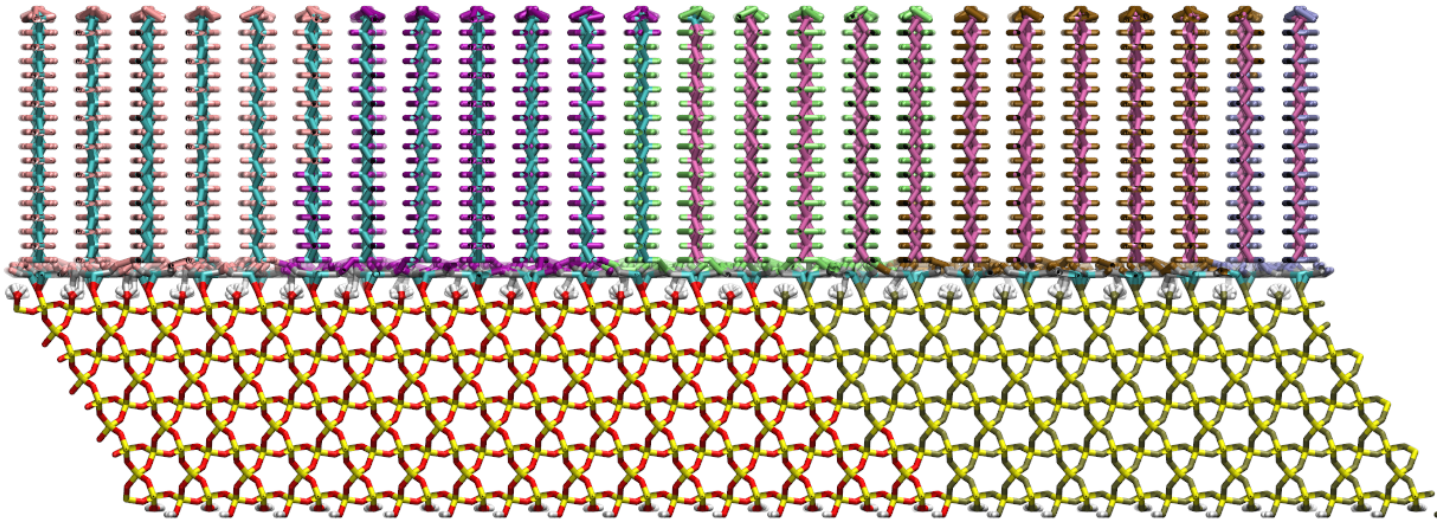

What is the **tilt angle** (inclination): Upright, slanted, or flat?

How does it depend the **coverage** of the substrate by silane?

What is the **layer thickness**? How **rough** is the top surface?

Silane self-assembled monolayers on silica

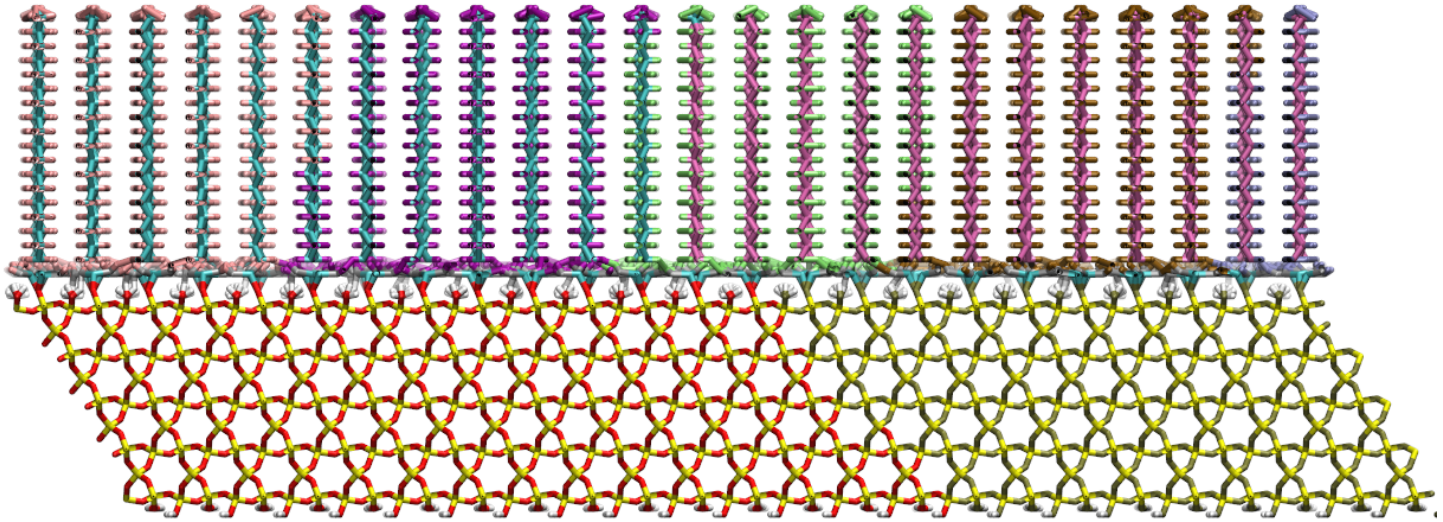

[1]J. M. Castillo, M. Klos, K. Jacobs, M. Horsch, H. Hasse, *Langmuir* 31(9), 2630 – 2638, **2015**.

Molecular dynamics simulation of silica covered with silane[1]

OPLS-AA, extended for silica,[2] substrate-substituent interaction is varied.

Surface oxygen atoms are bonded to silane (DTS/OTS), coverage is varied.

[2]B. W. Ewers, D. Batteas, *J. Phys. Chem. C* 116, 25165, **2012**.

Correlation: Coverage, tilt angle, thickness

β-cristobalite

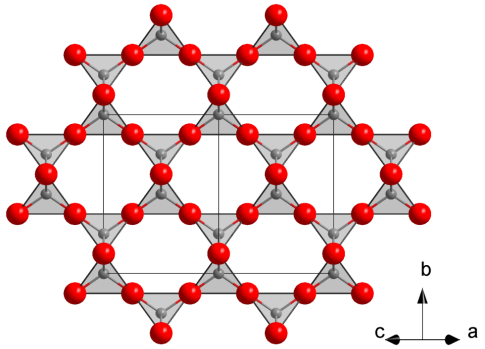

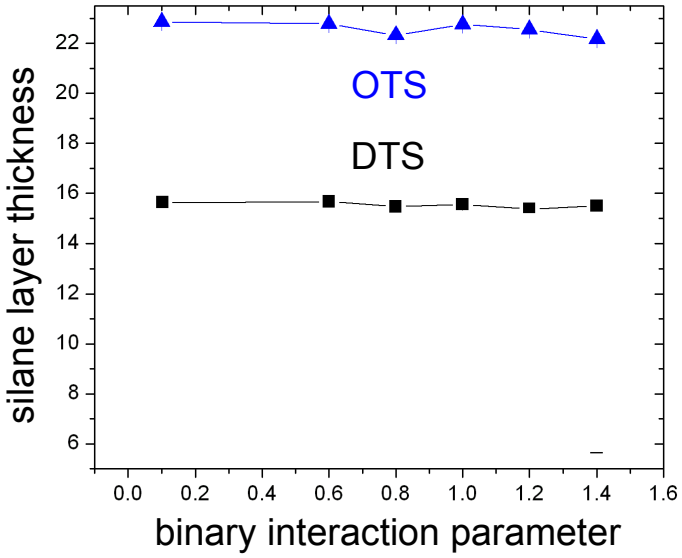

T = 298 K

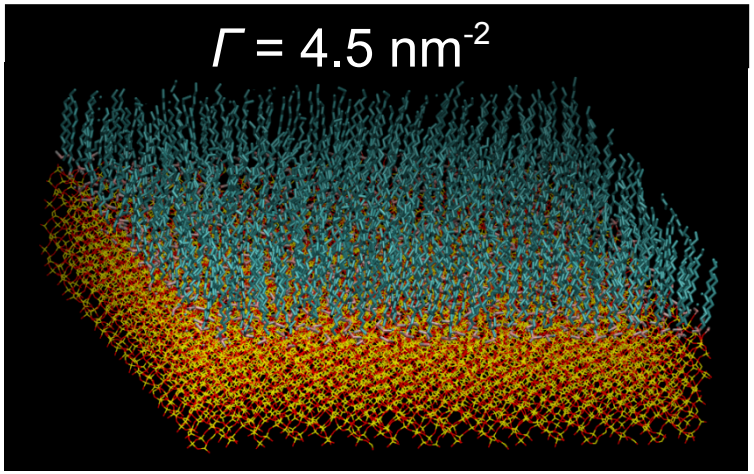

Castillo *et al.*, *Langmuir* 31, 2630, **2015**.

Correlation: Coverage, tilt angle, thickness

β-cristobalite

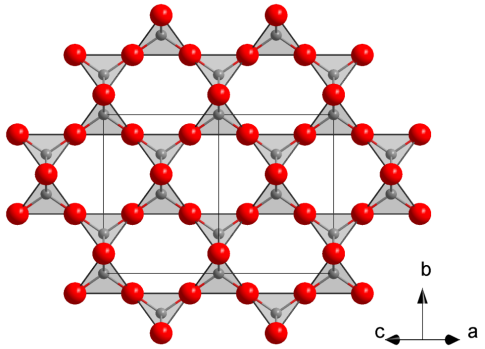

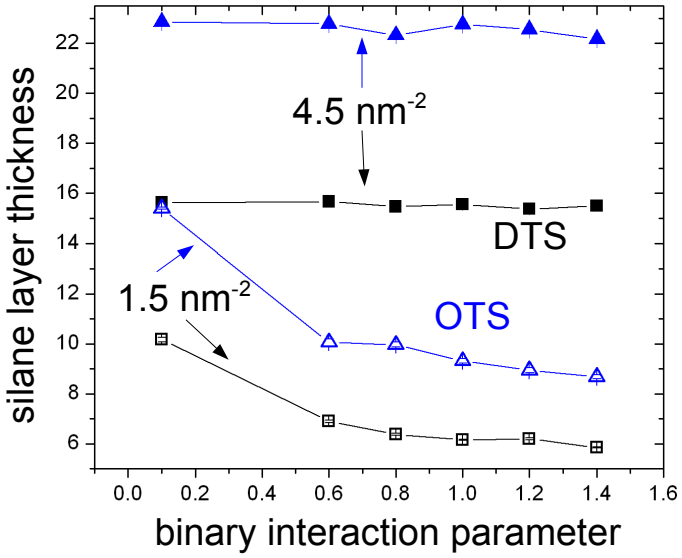

T = 298 K

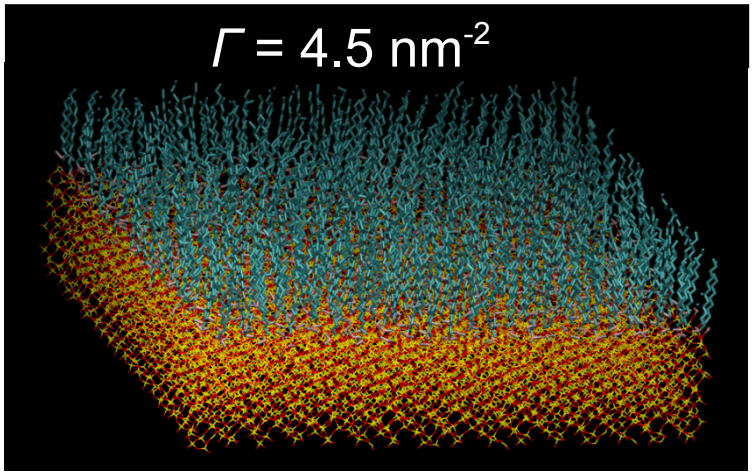

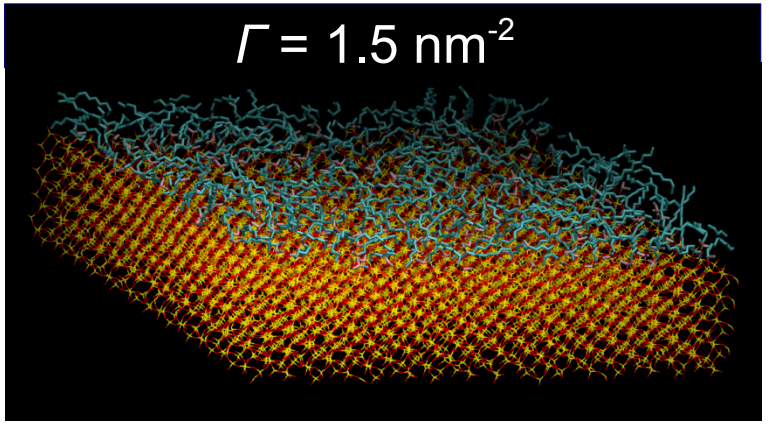

Surface morphology and dynamic wetting

Contact line pinning due to the structure of the three-phase contact region causes the deviation between advancing and receding contact angles.

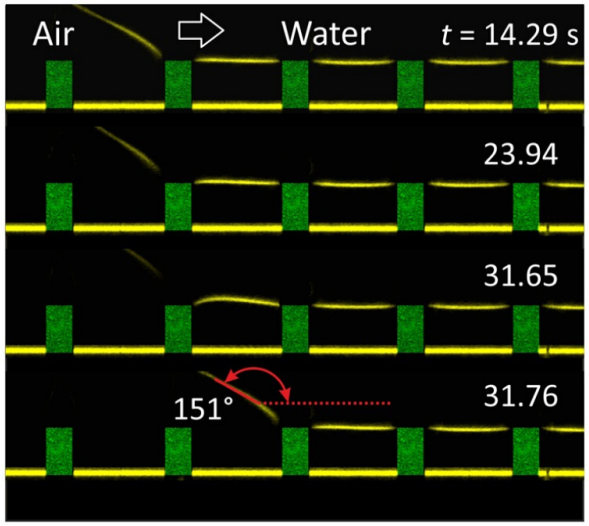

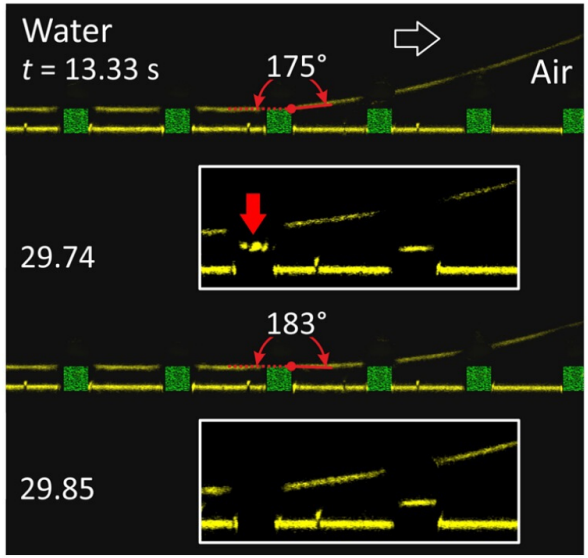

F. Schellenberger *et al.*, *Phys. Rev. Lett.* 116, 096101, **2016**

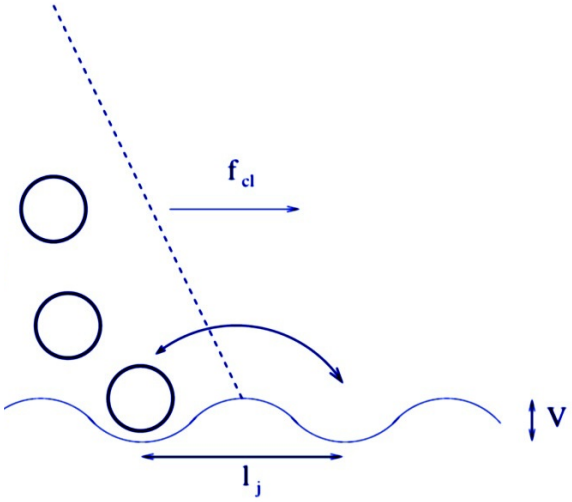

D. Bonn *et al.*, *Rev. Mod. Phys.* 81, 739, **2009**

Physical and chemical inhomogeneities are decisive for dynamic wetting.

Contact line pinning at an edge

Epitaxial Cassie state

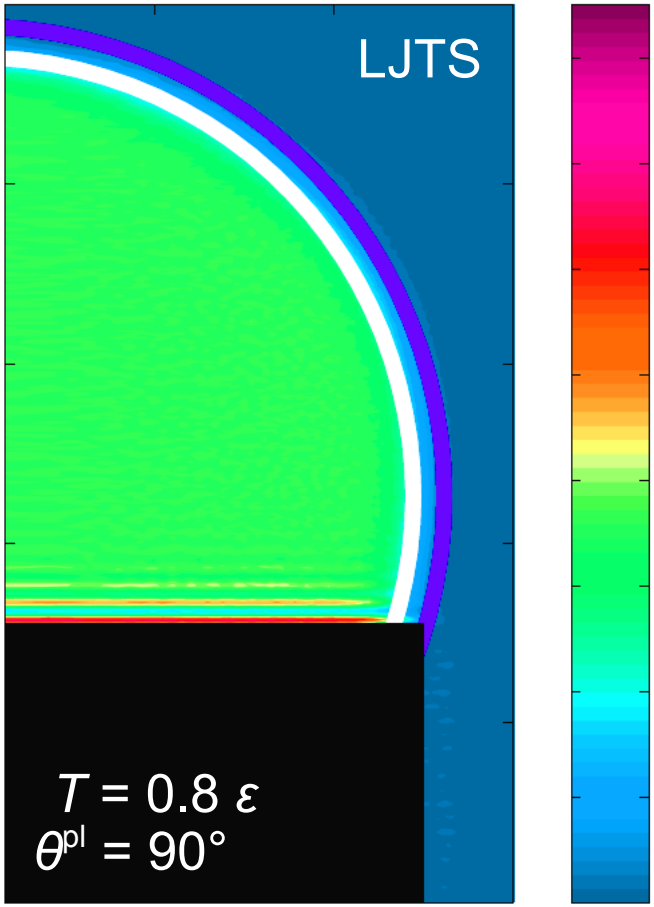

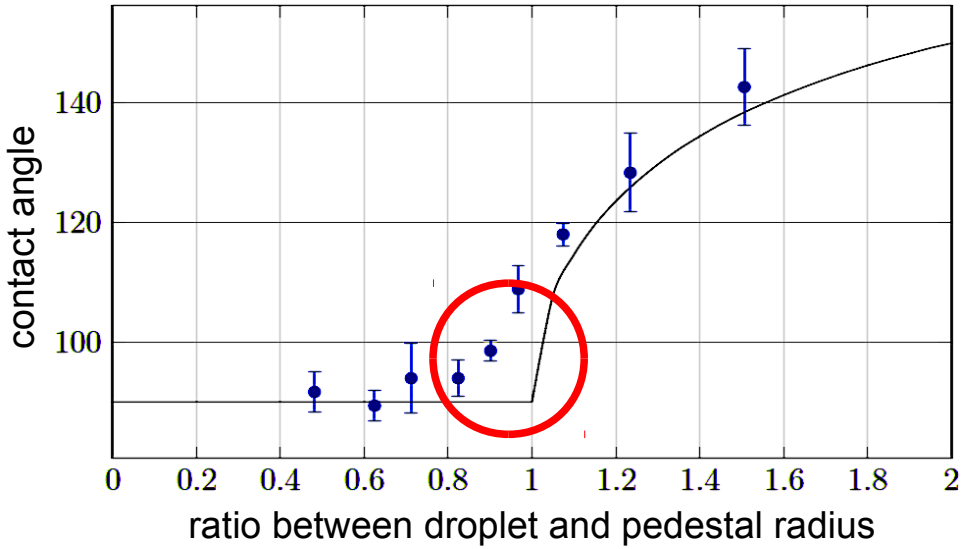

Line pinning does not occur exactly at the edge. The contact line is shifted inward due to the presence of a precursor layer.

Dynamic wetting: Spontaneous transition

Gibbs inequality:

$$\theta_0 \leq \theta \leq \theta_0 + \alpha$$

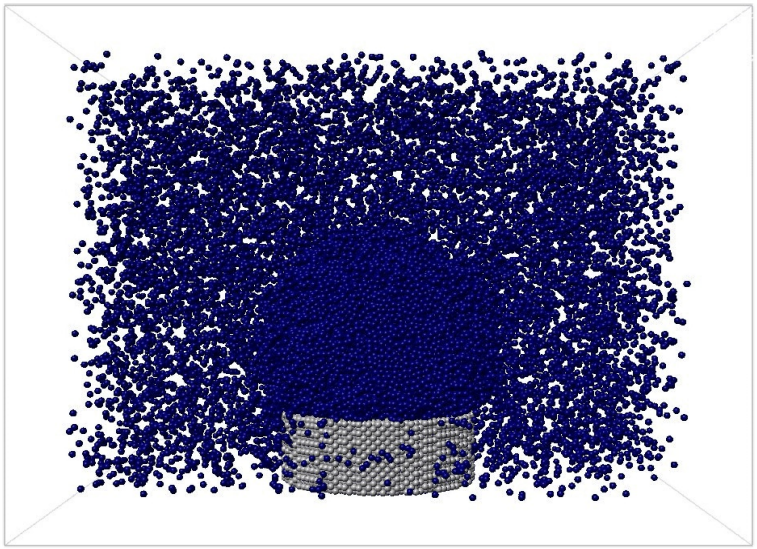

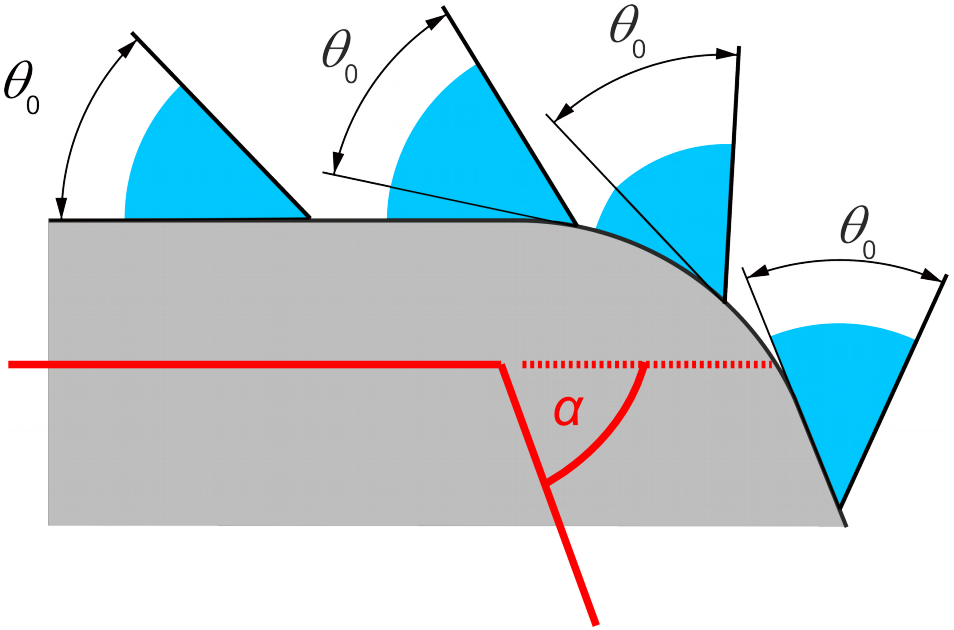

Dynamic wetting: Spontaneous transition

Case with $\theta^{max} = 180°$

Case with $\theta^{max} < 180°$

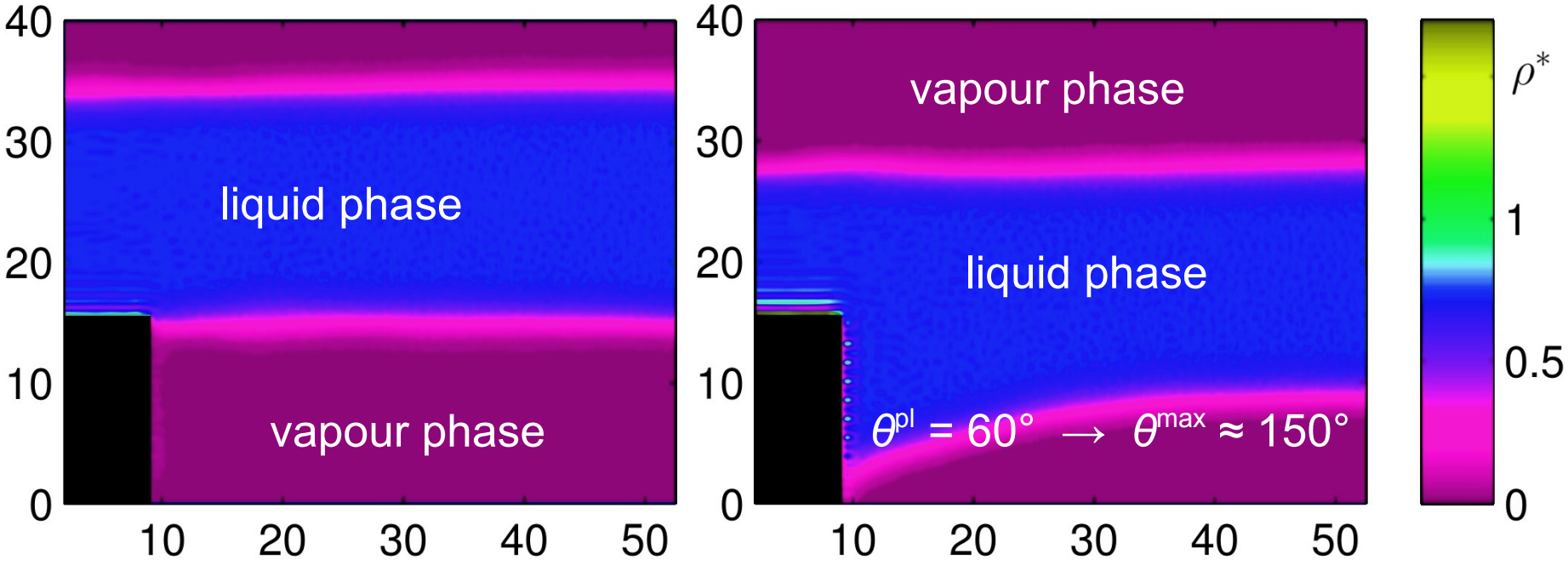

Present simulation results are in agreement with the Gibbs inequality.

Dynamic wetting: Activated transition

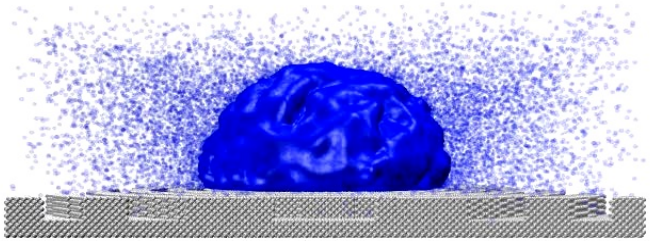

Contact line motion from one groove to the next is an activated process.

Dynamic wetting: Activated transition

Preferred mechanism at a nanostructured surface:

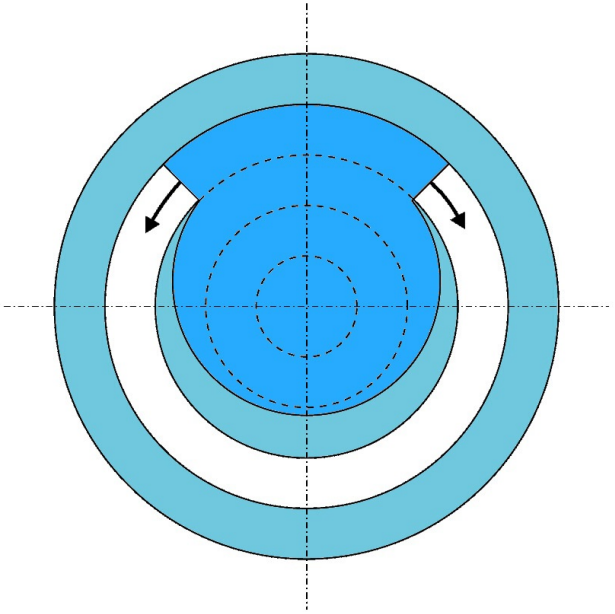

1. Expansion of the droplet in **radial direction** by nucleation of a bridge between two impregnated areas[1]
2. Complete or partial filling of the next groove by expansion of the droplet in **axial direction**

The present MD simulations confirm that dynamic wetting on nanostructured surfaces follows the mechanism proposed by de Gennes.[1]

[1]P. G. de Gennes, *Rev. Mod. Phys.* 57, 827, **1985**.

Scale bridging by mesoscopic approaches

Relaxation simulations based on a square-gradient **phase field model**:[1]

Allen-Cahn

$$\dot{\varphi} = -M \nabla_{\varphi} A$$

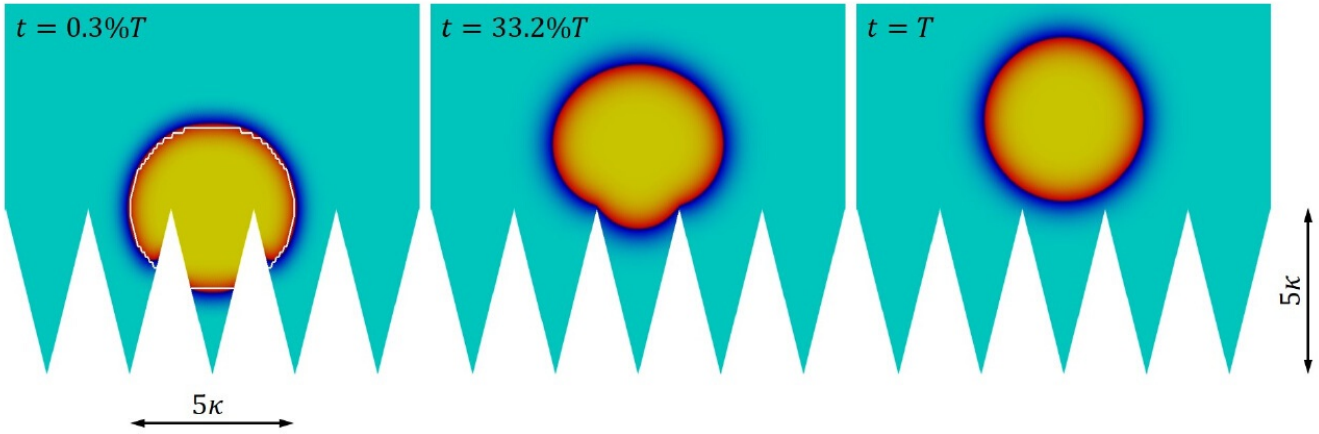

Future aims:

- Include inertia, external driving forces, non-equilibrium steady states
- Consider fluctuations, e.g. on the basis of fluctuating hydrodynamics

[1]F. Diewald, C. Kuhn, R. Blauwhoff, M. Heier, S. Becker, S. Werth, M. Horsch, H. Hasse, and R. Müller, *Proc. Appl. Math. Mech.* 16, 519, **2016**.

Conclusion

Scalable molecular simulation permits the crossover from the nanoscale to the microscale for large heterogeneous systems, while for thermodynamic properties of homogeneous systems, fast response times can be reached.

For the LJTS model, the dependence of the Young (planar) contact angle on the fluid-solid interaction, temperature, and solid density was determined. The results apply to many systems with dispersive interactions.

At a nanostructured surface, the deviation between the observed contact angle and the Young contact angle is (qualitatively) incorrectly described by Cassie and Wenzel model predictions.

Spontaneous and activated modes of dynamic wetting were considered by MD simulation. Nucleation of a bridge, as proposed by de Gennes, becomes the dominant mechanism when the structures are small.